[AMERICAN JOURNAL OF SCIENCE, VOL. 280, SUMMER, 1980, P. 575-606]

American Journal of Science

SUMMER 1980

DESCRIPTION AND INTERPRETATION OF METASOMATIC PHASE RELATIONS AT HIGH PRESSURES AND TEMPERATURES: 1. EQUILIBRIUM ACTIVITIES OF IONIC SPECIES IN NONIDEAL MIXTURES OF CO_2 AND H_2O

JOHN V. WALTHER* and HAROLD C. HELGESON

Department of Geology and Geophysics,
University of California, Berkeley, California 94720

ABSTRACT. Correlation of ionic activity diagrams incorporating explicit provision for solvation of aqueous species with temperature–X_{CO_2} diagrams depicting equilibrium among minerals and fluids in the system CaO–MgO–SiO_2–HCl–CO_2–H_2O facilitates thermodynamic analysis of multivariant high pressure/temperature phase relations in siliceous dolomites. Comparative calculations indicate that solvation and nonideal mixing in the system CO_2–H_2O may have a dramatic effect on the equilibrium activities and total concentrations of ionic species in fluids coexisting with calc-silicate mineral assemblages. Under certain circumstances the concentration of calcium in these fluids probably exceeds by several orders of magnitude the concentration of magnesium, which may then be essentially conserved among solids during metasomatic reaction of the fluid phase with its mineralogic environment. Application of activity diagrams to metamorphic systems affords a comprehensive basis for correlating field and laboratory observations with fluid inclusion studies and the solution chemistry of metamorphic fluids at high pressures and temperatures.

INTRODUCTION

Although temperature, pressure, and the mole fraction of CO_2 in fluids have been used extensively to describe and interpret phase relations in metamorphic rocks, few attempts have been made to correlate these variables with equilibrium activities of other species in the fluid phase. Such correlation facilitates thermodynamic analysis of metasomatic phase relations and affords the means to discriminate among dependent and independent variables in geochemical processes. Despite the fact that the bulk of the mineral assemblages in metamorphic rocks are multivariant, most petrologic studies focus on invariant, univariant, and/or divariant equilibria, which are commonly portrayed on temperature–X_{CO_2} diagrams. As a result, attention is drawn to decarbonation/dehydration processes and mineral assemblages consisting of large numbers of coexisting phases. However, the descriptive variables in temperature–X_{CO_2} diagrams do not necessarily coincide with their causal counterparts in the geochemical processes responsible for univariant and divariant mineral assemblages, which in most cases represent the end result of a series of multivariant reactions. The purpose of the present communication is to provide a theoretical framework for thermodynamic analysis

* Present address: Department of Geological Sciences, Northwestern University, Evanston, Illinois 60201

of such reactions by correlating logarithmic activity diagrams with their temperature–X_{CO_2} counterparts at high pressures and temperatures.

Metasomatism of siliceous dolomites is commonly ascribed to dehydration/decarbonation reactions accompanying burial or igneous intrusion, but it is now becoming evident that such reactions are inadequate in themselves to explain many of the mineralogic changes observed in calc–silicate rocks. A number of attempts have been made to document the extent to which metasomatic processes are isochemical (for example, Carmichael, 1969; Hewitt, 1973; Hutcheon and Moore, 1973; Morgan, 1975; Trommsdorff, 1972; Vidale and Hewitt, 1973; Carswell, Curtis, and Kanaris-Sotiriou, 1974; Poty, Stalder, and Weisbrod, 1974; Weisbrod and Poty, 1975; Moore and Kerrick, 1976; Kerrick, 1977; Touret, 1977; Mercolli, ms; Frisch and Helgeson, 1980). Although in some instances the relative degree to which components other than CO_2 and H_2O are involved in metasomatic processes remains uncertain, in others there is no doubt that the fluid phase introduced and/or removed SiO_2, MgO, CaO, Na_2O, K_2O, and even in some cases Al_2O_3. These observations are supported by correlation of thermodynamic calculations and experimental data with phase relations observed in the field (Hemley and others, 1977a and b, 1980; Frisch and Helgeson, 1980), which also indicates that many of the mineralogic changes observed in metamorphic rocks cannot be attributed simply to temperature/pressure gradients and dehydration/decarbonation reactions.

The role of aqueous electrolytes in metasomatic processes has received considerable attention in recent years, both from a theoretical (Helgeson, 1967a and b, 1968, 1969, 1970a and b; Helgeson, Brown, and Leeper, 1969; Eugster, 1970; Wintsch, 1975) and experimental (Hemley, 1959, 1967; Hemley and Jones, 1964; Hemley and others, 1971, 1977a and b, 1980; Orville, 1963, 1972; Ellis, 1963, 1968, 1969; Barnes and Ernst, 1963; Iiyama, 1964, 1966, 1970; Althaus and Johannes, 1969; Anderson and Burnham, 1967; Poty, Holland, and Borcsik, 1972; Frantz and Eugster, 1973; Shade, 1974; Chou and Eugster, 1977; Chou and Frantz, 1977; Frantz and Popp, 1977, 1979; Gunter and Eugster, 1978; and others) standpoint. Logarithmic activity diagrams generated from the thermodynamic properties of these electrolytes are commonly used to characterize quantitatively mineral equilibria in terms of the activities of ionic species in aqueous solutions responsible for diagenetic and hydrothermal processes (for example, Garrels, 1954; Hemley, 1959; Helgeson, 1964, 1967, 1970a and b; Garrels and Christ, 1965; Hess, 1966; Ellis, 1969; Helgeson, Garrels, and Mackenzie, 1969; Helgeson and Mackenzie, 1970). However, application of such diagrams to metamorphic systems has so far been largely qualitative (Eugster, 1970; Wintsch, 1975).

Recent theoretical research concerned with high pressure/temperature solution chemistry (Helgeson and Kirkham, 1974, 1976; Helgeson, Kirkham, and Flowers, in press; Helgeson, 1980; Walther and Helgeson, 1977; Delaney and Helgeson, 1978; McKenzie and Helgeson, 1979) and the thermodynamic properties of minerals (Helgeson and others, 1978)

permits construction of internally consistent activity diagrams for metamorphic systems at pressures and temperatures to 5 kb and 600°C. Because these diagrams are consistent with both experimental and observed phase relations, they can be used to characterize quantitatively the chemical interaction of mineral assemblages and aqueous electrolyte solutions in a wide variety of metasomatic processes.

Standard state conventions.—The standard state for minerals and H_2O_{liquid} adopted in the present study is one of unit activity of the pure solid or liquid at any pressure and temperature, but for CO_2 and H_2O_{gas} it calls for unit fugacity of the hypothetical ideal gas at 1 bar and any temperature. As a consequence, the activities of components corresponding to stoichiometric minerals and pure H_2O_{liquid} are unity, and the activities of CO_2 and H_2O_{gas} are equal to their fugacities at all pressures and temperatures. The standard state for aqueous species other than H_2O is defined as unit activity of the species in a hypothetical one molal solution referenced to infinite dilution at any pressure and temperature. Therefore, as the activity of the solvent (relative to the liquid standard state) approaches unity, the activity coefficients of aqueous species approach one at all pressures and temperatures. In contrast, as the mole fraction of a gas approaches unity at a given pressure and temperature, the fugacity coefficient of the gas approaches the value of the fugacity coefficient of the pure gas, which is not necessarily unity.

CONSTRAINTS ON ACTIVITY DIAGRAMS FOR SYSTEMS INVOLVING CO_2-RICH AQUEOUS FLUIDS

The thermodynamic basis and geologic application of activity diagrams have been summarized in a number of publications (see, for example, Garrels and Christ, 1965; Helgeson, 1968; Helgeson, Brown, and Leeper, 1969; Eugster, 1970; Kwak, 1971a and b; Vidale and Hewitt, 1973; Gunter and Eugster, 1978; Hemley and others, 1977a and b, 1980). However, in most of these the activity of H_2O (a_{H_2O}) is taken to be unity,

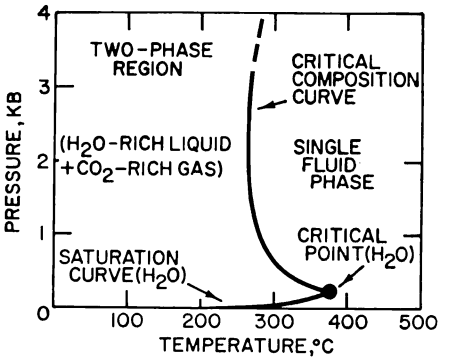

Fig. 1. Phase relations in the system CO_2–H_2O at high pressures and temperatures computed from data reported by Tödheide and Franck (1963) by Helgeson and others (1978).

which restricts the applicability of the diagrams to geochemical processes involving aqueous solutions with little or no dissolved CO_2. Despite the presence of relatively high concentrations of electrolytes in such solutions, the activity of H_2O is commonly close to unity, even at high pressures and temperatures (Helgeson, 1967b, 1969, 1980). In contrast, the activity of H_2O in fluids at temperatures above those corresponding to the miscibility gap in the system CO_2–H_2O (fig. 1) may depart appreciably from unity with increasing CO_2 concentration, which affects significantly both the intercepts and slopes of stability field boundaries on conventional activity diagrams representing dehydration/decarbonation equilibria.

Ion solvation and the activity of H_2O.—As emphasized recently by Hemley and others (1977b), generation of activity diagrams for systems in which a_{H_2O} departs significantly from unity requires explicit provision for solvation of the aqueous species involved in the reactions represented by the stability field boundaries on the diagram. This can be demonstrated by representing equilibrium among tremolite, talc, and an aqueous phase with the reaction,

$$\underset{(tremolite)}{Ca_2Mg_5Si_8O_{22}(OH)_2} + Mg^{++} \cdot (n_{Mg^{++}}\, H_2O) + 2\, H^+ \cdot (n_{H^+}\, H_2O) \rightleftharpoons$$

$$\underset{(talc)}{2\, Mg_3Si_4O_{10}(OH)_2} + (2\, n_{H^+} + n_{Mg^{++}} - 2\, n_{Ca^{++}})\, H_2O + 2\, Ca^{++} \cdot (n_{Ca^{++}}\, H_2O) \qquad (1)$$

where n_{H^+}, $n_{Mg^{++}}$, and $n_{Ca^{++}}$ represent the solvation numbers of the subscripted species.[1] It can be seen by inspection of reaction (1) that explicit provision for solvation of the ionic species introduces a reaction coefficient for H_2O, which is not true if the reaction is written as

$$\underset{(tremolite)}{Ca_2Mg_5Si_8O_{22}(OH)_2} + Mg^{++} + 2\, H^+ \rightleftharpoons \underset{(talc)}{2\, Mg_3Si_4O_{10}(OH)_2} + 2\, Ca^{++} \qquad (2)$$

Reaction (2) is a "shorthand" statement of reaction (1). It is not meant to imply that Mg^{++}, H^+, and Ca^{++} are not solvated, nor that there is no net change in the number of solvated H_2O dipoles associated with the reaction. The conventional values of the thermodynamic properties of ionic species in aqueous solution apply to formation of the solvated species. As such, they take into account implicitly the solvation process. For example, if we denote the (fictive) unsolvated aqueous hydrogen, magnesium, calcium, and chloride ions by $H.^+$, $Mg.^{++}$, $Ca.^{++}$, and $Cl.^-$, reaction (1) can be viewed as the sum of

$$\underset{(tremolite)}{Ca_2Mg_5Si_8O_{22}(OH)_2} \rightleftharpoons 2\, Ca_{(c)} + 5\, Mg_{(c)} + 8\, Si_{(c)} + 12\, O_{2(g)} + H_{2(g)} \qquad (3)$$

[1] Representation of solvated aqueous species as (for example) $Mg^{++} \cdot (n_{Mg^{++}}H_2O)$ rather than $Mg(H_2O)_{n_{Mg^{++}}}{}^{++}$ or $Mg(OH_2)_{n_{Mg^{++}}}{}^{++}$ is intended to imply weaker coordination of H_2O dipoles than other ligands in aqueous complexes by analogy with "zeolitic" or loosely bound H_2O molecules in minerals such as analcime ($NaAlSi_2O_6 \cdot H_2O$).

$$6\ Mg_{(c)} + 8\ Si_{(c)} + 12\ O_{2(g)} + 2\ H_{2(g)} \rightleftharpoons 2\ \underset{(talc)}{Mg_3Si_4O_{10}(OH)_2} \tag{4}$$

$$2\ H_{*}^{+} + 2\ Cl_{*}^{-} \rightleftharpoons H_{2(g)} + Cl_{2(g)} \tag{5}$$

$$2\ H^{+} \cdot (n_{H^{+}}\ H_2O) + 2\ Cl^{-} \cdot (n_{Cl^{-}}\ H_2O) \rightleftharpoons 2\ H_{*}^{+} + 2\ n_{H^{+}}\ H_2O_{(l)} + 2\ Cl_{*}^{-} + 2\ n_{Cl^{-}}\ H_2O_{(l)} \tag{6}$$

$$2\ Ca_{(c)} + 2\ Cl_{2(g)} \rightleftharpoons 2\ Ca_{*}^{++} + 4\ Cl_{*}^{-} \tag{7}$$

$$2\ Ca_{*}^{++} + 2\ n_{Ca^{++}}\ H_2O_{(l)} + 4\ Cl_{*}^{-} + 4\ n_{Cl^{-}}\ H_2O_{(l)} \rightleftharpoons 2\ Ca^{++} \cdot (n_{Ca^{++}}\ H_2O) + 4\ Cl^{-} \cdot (n_{Cl^{-}}\ H_2O) \tag{8}$$

$$2\ Cl_{*}^{-} + Mg_{*}^{++} \rightleftharpoons Mg_{(c)} + Cl_{2(g)} \tag{9}$$

and

$$Mg^{++} \cdot (n_{Mg^{++}}\ H_2O) + 2\ Cl^{-} \cdot (n_{Cl^{-}}\ H_2O) \rightleftharpoons Mg_{*}^{++} + n_{Mg^{++}}\ H_2O_{(l)} + 2\ Cl_{*}^{-} + 2\ n_{Cl^{-}}\ H_2O_{(l)} \tag{10}$$

where the subscripts (*c*), (*g*), and (*l*) refer to the crystalline, gas, and liquid states, respectively. The conventional standard molal Gibbs free energies of formation from the elements in their stable form at 25°C and 1 bar (ΔG°_{f}) of $H^{+} \cdot (n_{H^{+}}\ H_2O)$, 0.5 $Ca^{++} \cdot (n_{Ca^{++}}\ H_2O)$, and 0.5 $Mg^{++} \cdot (n_{Mg^{++}}\ H_2O)$ are equal to one half the negative sum of the molal Gibbs free energy changes associated with reactions (5) and (6), one fourth the sum of the molal Gibbs free energy changes for reactions (7) and (8), and one half the negative sum of the corresponding changes for reactions (9) and (10), respectively, minus the standard molal Gibbs free energy of formation from the elements of dissociated $HCl_{(aq)}$, which corresponds to one half the negative sum of the molal Gibbs free energy changes for reactions (5) and (6).[2]

Nevertheless, these species are commonly written as H^{+}, Ca^{++}, and Mg^{++}. Reactions (1) and (2) are thus equivalent, as are their thermodynamic properties. However, the law of mass action expressions for the two reactions are equivalent only if $a_{H_2O} = 1$. This can be demonstrated by comparing logarithmic statements of the law of mass action for reactions (1) and (2), which can be written for

$$a_{Ca_2Mg_5Si_8O_{22}(OH)_2} = a_{Mg_3Si_4O_{10}(OH)_2} = 1$$

as

$$\log ((a_{Ca^{++}} \cdot (n_{Ca^{++}}\ H_2O))/(a_{H^{+}} \cdot (n_{H^{+}}\ H_2O))^2) = 0.5\ (\log ((a_{Mg^{++}} \cdot (n_{Mg^{++}}\ H_2O))/(a_{H^{+}} \cdot (n_{H^{+}}\ H_2O))^2) + \log K - (2n_{H^{+}} + n_{Mg^{++}} - 2n_{Ca^{++}}) \log a_{H_2O}) \tag{11}$$

and

$$\log (a_{Ca^{++}}/a_{H^{+}}^2) = 0.5\ (\log (a_{Mg^{++}}/a_{H^{+}}^2) + \log K), \tag{12}$$

[2] It thus follows that $\Delta G^{\circ}_{f,H^{+} \cdot (n_{H^{+}}\ H_2O)} = 0$, and $\Delta G^{\circ}_{f,Cl^{-} \cdot (n_{Cl^{-}}\ H_2O)} = \Delta G^{\circ}_{f,dissociated\ HCl_{(aq)}}$.

respectively, where K represents the equilibrium constants for reactions (1) and (2), which are identical. It can be seen by inspection that eq (12) is a valid "shorthand" proxy for eq (11) only if $a_{H_2O} = 1$. In all other cases, eq (12) is both misleading and incorrect, as are activity diagrams generated from it or its analogs for other reactions.

Equation (11) can be written in abbreviated notation as

$$\log (a_{Ca^{++}}/a_{H^+}{}^2) = 0.5 (\log (a_{Mg^{++}}/a_{H^+}{}^2) + \log K - (\Delta n_{Mg^{++}} - 2\Delta n_{Ca^{++}}) \log a_{H_2O}) \quad (13)$$

where

$$\Delta n_{Mg^{++}} \equiv n_{Mg^{++}} - 2n_{H^+} \quad (14)$$

and

$$\Delta n_{Ca^{++}} \equiv n_{Ca^{++}} - 2n_{H^+} \quad (15)$$

which can be generalized for any reversible reaction among stoichiometric minerals and an aqueous phase to give

$$\sum_i \hat{n}_{i,r} \log (a_i/a_{H^+}{}^{Z_i}) = \log K_r + \sum_i \hat{n}_{i,r} \Delta n_i \log a_{H_2O} \quad (16)$$

where Z_i denotes the charge on the ith aqueous species other than H^+ ($i = 1,2, \ldots \hat{i}$), a_i, a_{H^+}, and a_{H_2O} refer to the activities of the subscripted (solvated) species in the aqueous phase, K_r represents the equilibrium constant for the rth reaction, $\hat{n}_{i,r}$ stands for the reaction coefficient of the subscripted species in the reaction, which is positive for products and negative for reactants, and

$$\Delta n_i \equiv n_i - Z_i n_{H^+} \quad (17)$$

Note that the subscript i in eq (16) also applies to H_2O ($\Delta n_{H_2O} = n_{H_2O} = 1$), which provides for the appearance in the reaction of H_2O derived from minerals.

Reliable activity diagrams can be generated with the aid of eq (16) for systems in which $a_{H_2O} \neq 1$. If values of Δn_i are known for all values of i, the right side of the equation can be evaluated, and log $(a_i/a_{H^+}{}^{Z_i})$ can be used as descriptive variables in the diagrams. However, if this is not the case and $a_{H_2O} \neq 1$, the descriptive variables become log $(a_i/(\sigma_i\, a_{H^+}{}^{Z_i}))$, where

$$\sigma_i \equiv a_{H_2O}{}^{\Delta n_i} \quad (18)$$

Regardless of whether σ_i is constant, phase relations in geologic systems can be portrayed accurately on activity diagrams cast in terms of log $(a_i/\sigma_i\, a_{H^+}{}^{Z_i})$. However, calculation of log $(a_i/a_{H^+}{}^{Z_i})$ from values of these descriptive variables requires values of a_{H_2O} and Δn_i. The activity of H_2O can usually be calculated and realistic values specified for a given diagram. In contrast, reliable solvation numbers are not available for aqueous species at high pressures and temperatures, nor can they be computed with confidence from experimental data so far reported in the literature. Nevertheless, until such data become available, activity diagrams for

systems in which a_{H_2O} is significantly less than unity can be cast in terms of log $(a_i/(\sigma_i\ a_{H^+}{}^{z_i}))$, which affords an accurate and comprehensive framework for description and interpretation of phase relations in geologic systems.

The significance of the term "solvation number" has been the subject of considerable discussion in the literature (see, for example, Bockris, 1949; Journet and Vadon, 1955; Mikhailov and Drakin, 1960; Conway, 1966; Desnoyers and Jolicoeur, 1969; Friedman and Krishnan, 1973; Hepler and Woolley, 1973; Samoilov, 1957, 1972; Ling, 1972; Prue, 1966; Frank, 1966; Muirhead-Gould and Laidler, 1966; Kavanau, 1964; Nightingale, 1966; Bockris, Saluja, and Madan, 1970), which contains nearly as many different sets of contradictory solvation numbers as there are methods of deriving them. Ion solvation is a statistical concept that refers to the reduced orientational polarizability of H_2O dipoles in the vicinity of an ion. However, these dipoles, which may be temporarily in primary, secondary, or higher order coordination, rapidly and continually exchange position with other dipoles in the bulk fluid. The *average* number of H_2O dipoles that are affected by the presence of an ion at any given instant of time corresponds to the solvation number for the ion. The solvation process for an ion with a given charge and effective electrostatic radius is controlled by the dielectric constant of the solvent, which in the case of H_2O decreases dramatically with increasing temperature and/or decreasing pressure at high temperatures (Helgeson and Kirkham, 1974, 1976; Helgeson, Kirkham, and Flowers, in press). It would therefore be reasonable to expect σ_i to approach unity at high temperatures.

Decreased ion solvation at high temperatures is consistent with the observation that the extended term parameter in the Hückel equation (b_γ) exhibits a maximum as a function of temperature. At pressures corresponding to those along the vapor-liquid equilibrium curve for H_2O and temperatures >50° to 200°C, depending on the electrolyte, b_γ decreases dramatically with increasing temperature and becomes negative at high temperatures (Helgeson, Kirkham, and Flowers, in press). This behavior implies decreasing ion solvation with increasing temperature above that corresponding to the extremum in b_γ as a function of temperature.

Permittivity studies of electrolyte solutions at low temperatures indicate that H_2O dipoles in primary coordination about cations are "tightly" bound, but those in the immediate vicinity of anions are loosely held and easily perturbed. As temperature increases and the standard molal Gibbs free energy of solvation becomes less negative, cations (and even to a greater extent, anions) become less effective in retaining their "coordinated" dipoles, which favors replacement of solvated dipoles about cations by anions to form complexes such as NaCl, KCl, $MgCl_2$, et cetera. These species themselves may or may not occur in high concentrations or be solvated to form inner- and/or outer-sphere complexes, but the ions from which they form at high temperatures are almost certainly not solvated to anywhere near the degree they are at low temperatures.

Quartz solubility measurements in H_2O–Ar and H_2O–CO_2 mixtures suggest that solvation numbers for aqueous silica vary between 2 and 6 at pressures and temperatures from 1 to 5 kb and 500° to 900°C (Sommerfeld, 1967; Novgorodov, 1975; Shettel, ms). However, large uncertainties attend calculation of solvation numbers from experimental solubility measurements, and it is not clear to what extent the various solvation numbers reported for $SiO_{2(aq)}$ actually represent stepwise dissociation of $Si(OH)_4$ and/or H_2O–Ar and CO_2–H_2O association.

Ion association.—Although the logarithms of the activities of cations are commonly used as descriptive variables in activity diagrams, this practice is not meant to imply that dissociated species necessarily predominate in aqueous electrolyte solutions. In fact, ample evidence (which has been summarized by Helgeson, 1969; and Helgeson and Kirkham, 1976) indicates that increasing temperature and decreasing pressure at high temperature favors formation of complexes in hydrothermal solutions. The activities of species such as $Mg^{++} \cdot (n_{Mg^{++}}\ H_2O)$ and $Ca^{++} \cdot (n_{Ca^{++}}\ H_2O)$ in these solutions are related to those of complexes like $MgCl^+ \cdot (n_{MgCl^+}\ H_2O)$, $MgCl_2 \cdot (n_{MgCl_2}\ H_2O)$, $CaCl^+ \cdot (n_{CaCl^+}\ H_2O)$, and $CaCl_2 \cdot (n_{CaCl_2}\ H_2O)$ by appropriate statements of the law of mass action for the dissociation of the complexes. For example, reversible dissociation of $MgCl^+ \cdot (n_{MgCl^+}\ H_2O)$ can be written as

$$MgCl^+ \cdot (n_{MgCl^+}\ H_2O) \rightleftharpoons Mg^{++} \cdot (n_{Mg^{++}}\ H_2O) + Cl^- \cdot (n_{Cl^-}\ H_2O) + (n_{MgCl^+} - n_{Mg^{++}} - n_{Cl^-})\ H_2O \quad (19)$$

for which

$$\frac{a_{Mg^{++} \cdot (n_{Mg^{++}}\ H_2O)}\ a_{Cl^- \cdot (n_{Cl^-}\ H_2O)}\ a_{H_2O}^{(n_{MgCl^+} - n_{Mg^{++}} - n_{Cl^-})}}{a_{MgCl^+ \cdot (n_{MgCl^+}\ H_2O)}} = K \quad (20)$$

The activities of these various aqueous species are related to the composition of the solution by activity coefficients and charge and material balance equations, which can be used together with expressions of the form of eq (20) to relate ionic activity diagrams to fluid inclusion compositions at temperatures to 900°C (Helgeson, 1969, 1980; Helgeson, Kirkham, and Flowers, in press; McKenzie and Helgeson, 1979).

Nonideality in the system CO_2–H_2O.—Departures from ideality in the system CO_2–H_2O are depicted in figure 2, which was generated from Flowers' (1979) correction of Holloway's (1977) adaptation of the modified Redlich-Kwong algorithm for calculating high pressure/temperature fugacity coefficients of CO_2 and H_2O in CO_2–H_2O mixtures. Inspection of this figure reveals that Flowers' (1979) equations lead to relatively large departures from ideality in CO_2-rich fluids at 400°C and 2 kb where the calculated fugacity coefficients of CO_2 (χ_{CO_2}) in the mixture exceed by more than a factor of 2 the fugacity coefficients of pure CO_2. However, as temperature increases to ~600°C, the thermodynamic behavior of the fluid approaches ideality. The relations shown in figure 2 were used in the present study to calculate values of the fugacity of H_2O (f_{H_2O})

and f_{CO_2} from fluid compositions constrained by $X_{CO_2} + X_{H_2O} = 1$ at $P_{fluid} = P_{total}$.

It can be deduced from figure 2 that nonideality in the system CO_2–H_2O may have a dramatic effect on the intercepts of saturation limits and stability field boundaries on activity diagrams generated for a given pressure, temperature, and X_{CO_2}. For example, log $(a_i/\sigma_i\, a_{H^+}{}^{z_i})$ for equilibria involving carbonates in H_2O-rich fluids at 400°C may be affected by more than 0.8 $\hat{n}_{CO_2,r}$ (where $\hat{n}_{CO_2,r}$ represents the reaction coefficient of CO_2 in the rth reaction). Similarly, log $(a_i/\sigma_i\, a_{H^+}{}^{z_i})$ for dehydration equilibria involving CO_2-rich fluids at 400°C may vary by as much as 0.4 $\hat{n}_{H_2O,r}$. It follows that both the intercepts and slopes of univariant curves on temperature–X_{CO_2} and log $(a_i/(\alpha_i\ a_{H^+}{}^{z_i}))$ diagrams may be affected significantly by departures from ideality in the system CO_2–H_2O.

PHASE RELATIONS IN THE SYSTEM CaO–MgO–SiO_2–HCl–CO_2–H_2O

Metamorphism of siliceous dolomites has received considerable attention in recent years (Weeks, 1956; Harker and Tuttle, 1956; Metz and Winkler, 1963; Walter, 1965; Trommsdorff, 1966b, 1968, 1972; Newton, 1966; Melson, 1966; Metz, 1967, 1970; Greenwood, 1967; Metz and Trommsdorff, 1968; Shmulovich, 1969; Gordon and Greenwood, 1970; Gordon, 1971; Skippen, 1971, 1974; Hutcheon and Moore, 1973; Kridelbaugh, 1973; Cermignani and Anderson, 1973; Puhan and Hoffer, 1973; Hewitt, 1973; Kerrick, Crawford and Randazzo, 1973; Kerrick, 1974, 1977; Slaughter, Kerrick and Wall, 1974; Glassley, 1975; Morgan, 1975; Joesten, 1976; Moore and Kerrick, 1976; Rice, 1977; Trommsdorff and Evans, 1977; Kase and Metz, 1977), and solubility relations among calcium magnesian silicates and aqueous solutions have been documented both theoretically and experimentally (Hemley and others, 1977a and b; Walther and Helgeson, 1977; Helgeson and others, 1978; Gunter and Eugster, 1978; Frantz and Popp, 1979; McKenzie and Helgeson, 1979). As a consequence, calc–silicate rocks are particularly well suited for demonstrating the advantages of using activity diagrams to interpret phase relations resulting from metasomatic processes.

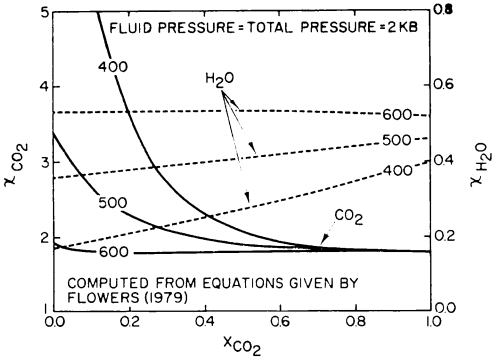

Fig. 2. Fugacity coefficients of CO_2 (solid lines) and H_2O (dashed lines) as a function of temperature (labeled in °C) and X_{CO_2} at 2 kb.

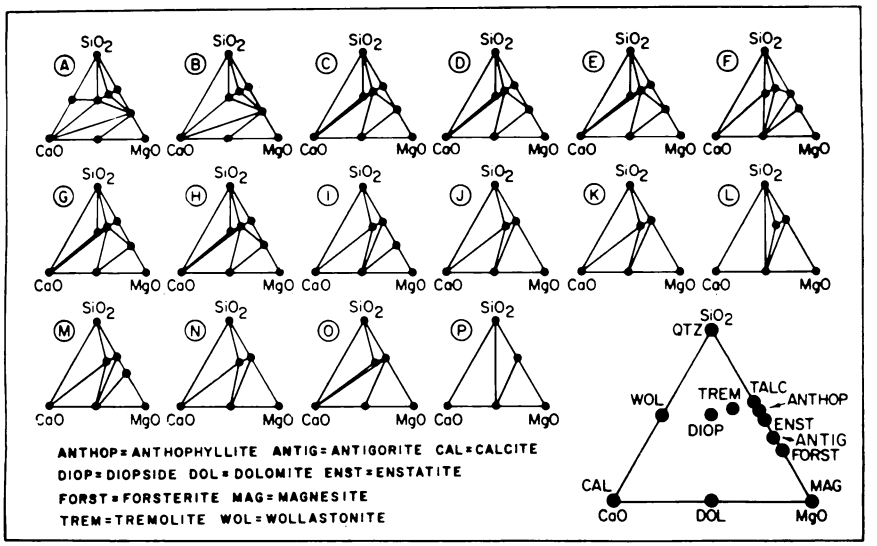

Fig. 3. Compositions, abbreviations and phase relations among minerals in the system CaO–MgO–SiO_2–H_2O–CO_2 at 2 kb. The circled letters correspond to those designating temperature–X_{CO_2} coordinates in figures 10 and 11 (see text).

The thermodynamic data and equations used to generate the diagrams shown below were taken from Helgeson and Kirkham (1974, 1976), Helgeson, Kirkham, and Flowers (in press), Flowers (1979), Walther and Helgeson (1977)[3], and Helgeson and others (1978). The compositions of the minerals considered in the present study, together with their abbreviations are shown in figure 3. Of the minerals in the system CaO–MgO–SiO_2–CO_2–H_2O, only calcite exhibits significant compositional variation at pressures and temperatures below 5 kb and 600°C. Accordingly, all minerals other than calcite were regarded as stoichiometric phases. Substitutional order/disorder in dolomite was taken into account with the aid of thermodynamic equations and data summarized by Helgeson and others (1978).

Calculation of the activity of $CaCO_3$ in magnesian calcite.—The activity of $CaCO_3$ in magnesian calcite coexisting with dolomite at high pressures and temperatures can be computed from (Gordon and Greenwood, 1970)

[3] Footnote *l* of table 1 in Walther and Helgeson (1977) contains a typographical error which should be corrected. Instead of 49.003 and 31.208 cal mole^{-1} (°K)$^{-1}$, the values shown in the footnote for the standard molal entropies of $Si_{(c)}$ and $O_{2(g)}$ should read 4.5 and 49.003 cal mole^{-1} (°K)$^{-1}$, respectively. In addition, eq (10) in the sentence preceding eq (25) should read eq (13), the second left parenthesis in the third term on the right side of eq (25) should be deleted, and the units of a_3 and c_1 on page 1330 should be corrected to read cal mole^{-1} bar^{-1} and cal mole^{-1} (°K)$^{-1}$, respectively. It should also be noted that all the calculations discussed above took into account typographical errors in a number of the equations given by Helgeson and Kirkham (1974, 1976), which are corrected in footnote 1 of Helgeson and Kirkham (1976), footnotes 1 and 2 of Walther and Helgeson (1977), footnote 1 of Delany and Helgeson (1978), and footnote 1 of Helgeson (1980).

$$ln\ a_{CaCO_3} = (1 - X_{CaCO_3})^2\ (1.2238 + 1.8960\ X_{CaCO_3}) + ln\ X_{CaCO_3} \quad (21)$$

for

$$X_{CaCO_3} + X_{MgCO_3} = 1 \text{ and } 0.82 \leqslant X_{CaCO_3} \leqslant 1.0.$$

Note that eq (21) is independent of both pressure and temperature. The equilibrium composition of magnesian calcite coexisting with dolomite at 2 kb can be expressed as

$$ln\ (1 - X_{CaCO_3}) = \frac{456.86}{T - 375} + 3.3183\ ln\ (T - 375) - 24.126, \quad (22)$$

which was generated in the present study by regression of the experimental data shown in figure 4. It can be shown that the composition of dolomite along the solvus departs negligibly from $X_{MgCO_3} = 0.5$ at 2 kb and temperatures below 600°C. As a consequence, the activity of $CaMg(CO_3)_2$ in dolomite coexisting with calcite can be taken as unity. Evaluation of eqs (21) and (22) together with statements of the law of mass action for calcite coexisting with other phases in the system CaO–MgO–SiO_2–HCl–CO_2–H_2O indicates that compositional variation in calcite below 600°C at 2 kb affects equilibrium temperatures by less than 1.5°C (mole of calcite in the reaction)$^{-1}$, which is equivalent to ~0.01 units in log $(a_i/(\sigma_i\ a_{H^+}{}^{Z_i}))$ at constant temperature.

Activity diagrams at constant pressure, temperature, and X_{CO_2}.—Activity diagrams are depicted in figures 5 through 8 for the system CaO–MgO–SiO_2–HCl–CO_2–H_2O at 2 kb and a series of temperatures and values of X_{CO_2}. The diagrams were generated from the equations and data cited above with provision for substitutional order/disorder in dolomite, compositional variation in calcite, solvation of aqueous species, and nonideality in the system CO_2–H_2O. The dashed lines on the diagrams represent saturation in the fluid phase of calcite (horizontal dashed lines), magnesite (vertical dashed lines), and dolomite (inclined dashed lines). All equilibria at values of log $(a_{Mg^{++}}/(\sigma_{Mg^{++}}\ a_{H^+}{}^2))$ and log $(a_{Ca^{++}}/(\sigma_{Ca^{++}}\ a_{H^+}{}^2))$ greater than those corresponding to the dashed lines are metastable. The circled letters in figures 5 through 8 correlate with those shown in figure 3, where equilibrium phase relations are depicted in terms of the mole fractions of CaO, MgO, and SiO_2.

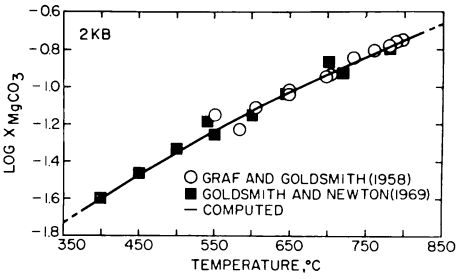

Fig. 4. Log X_{MgCO_3} in magnesian calcite as a function of temperature at 2 kb along the calcite–dolomite solvus (see text).

The phase relations shown in figures 5 through 8 and in subsequent figures are based in part on the assumption that additions of small concentrations of HCl to CO_2–H_2O fluids will not introduce a miscibility gap in the system at 2 kb and temperatures $\geqslant$400°C. Experimental pressure-temperature-composition data for the system H_2O–CO_2–NaCl at high pressures and temperatures (Gehrig, Lentz, and Franck, 1979; Franck, 1980) suggest by analogy that this assumption is probably valid only if the fluid is dilute with respect to HCl.

It can be deduced from figures 5 through 8 that most commonly observed mineral assemblages in quartz-deficient calc–silicate rocks coexist with a fluid phase in which log $(a_{Mg^{++}}/(\sigma_{Mg^{++}}\ a_{H^+}{}^2))$ and log $(a_{Ca^{++}}/(\sigma_{Ca^{++}}\ a_{H^+}{}^2))$ range over less than a log unit at constant temperature, pressure, and X_{CO_2}. Note that the trace of the intersection of the calcite and dolomite saturation lines as a function of X_{CO_2} at constant temperature is sub-parallel to the tremolite–talc and tremolite–diopside stability field boundaries. Hence, at certain pressures and temperatures where the intersection is near these boundaries, small changes in the

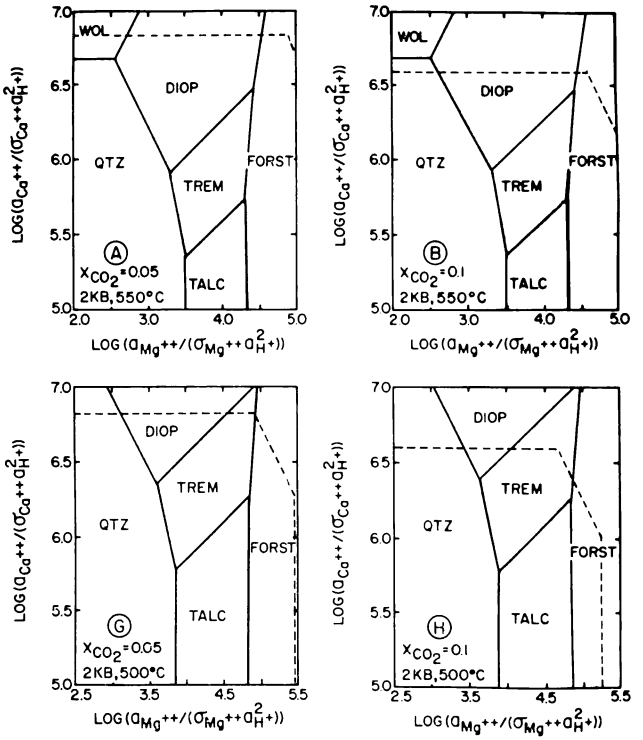

Fig. 5. Logarithmic activity diagrams for the system CaO–MgO–SiO_2–HCl–CO_2–H_2O at 2 kb and 500° and 550°C for X_{CO_2} = 0.05 and 0.1. The circled letters correspond to those designating temperature X_{CO_2} coordinates in figure 10. The dashed lines represent saturation in the fluid phase with respect to calcite (horizontal dashed lines), magnesite (vertical dashed lines), and dolomite (inclined dashed lines).

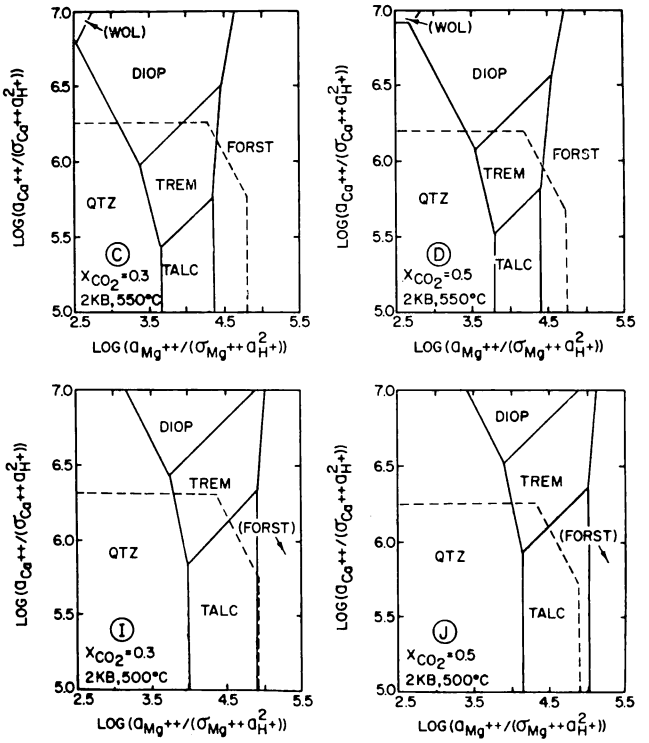

Fig. 6. Logarithmic activity diagrams for the system CaO–MgO–SiO_2–HCl–CO_2–H_2O at 2 kb and 500° and 550°C for X_{CO_2} = 0.30 and 0.50 (see caption of fig. 5).

relative stabilities of the minerals arising from solid solution may have a substantial effect on the range of X_{CO_2} over which talc, tremolite, and diopside coexist with calcite and dolomite. Note that at both low and high values of X_{CO_2}, log $(a_{Ca^{++}}/(\sigma_{Ca^{++}}\ a_{H^+}{}^2))$ for mineral assemblages containing dolomite and magnesite is higher than that for phase assemblages involving quartz, talc, and tremolite.

It can be deduced from figures 5 through 8 that if $\sigma_{Ca^{++}} \approx \sigma_{Mg^{++}}$ (which seems likely), $a_{Ca^{++}}$ is ~4 orders of magnitude greater than $a_{Mg^{++}}$ in H_2O-rich fluids coexisting with calcite, wollastonite, and diopside, or calcite, quartz, and diopside at 2 kb and temperatures $\geqslant$500°C. Because the dissociation constant of $CaCl_2$ is ~2 to 3 orders of magnitude greater than that of $MgCl_2$ at high temperatures (McKenzie and Helgeson, 1979), if the activity coefficients of $CaCl_2$ and $MgCl_2$ are close to unity and those of Ca++ and Mg++ are nearly the same for a given "true" ionic strength (Helgeson, Kirkham, and Flowers, in press), it follows that the total concentration of calcium in these fluids may be several orders of magnitude greater than that of magnesium. Fluid inclusion analyses (Poty and others, 1977) as well as the compositions of geothermal brines such as those in the Salton Sea geothermal system (Helgeson, 1968) sug-

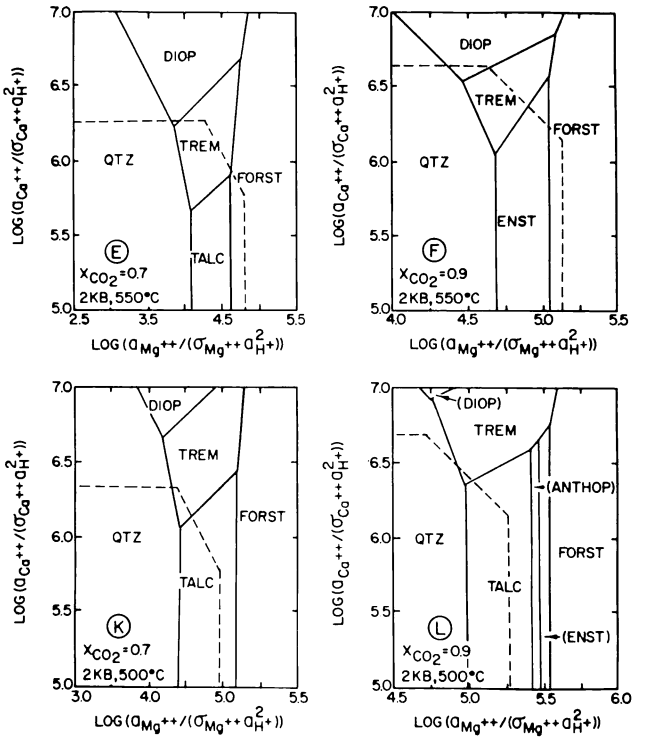

Fig. 7. Logarithmic activity diagrams for the system CaO–MgO–SiO_2–HCl–CO_2–H_2O at 2 kb and 500° and 550°C for X_{CO_2} = 0.70 and 0.90 (see caption of fig. 5).

gest that this conclusion is also valid for fluids coexisting with other mineral assemblages at lower temperatures.

The observations summarized above suggest that under certain circumstances the behavior of magnesium in geochemical processes is like that of aluminum, which is nearly conserved among reactant and product minerals during reaction of a fluid phase with its mineralogic environment. However, it is also true that if the magnesium concentration is small, it may change significantly during reaction, which would not be true of species present in relatively large concentrations. Fluid inclusion studies and geothermal brine analyses suggest that calcium chloride concentrations in solutions involved in metasomatic processes are of the order of 0.1 to 1 *m*. It thus appears that the chemical potential of calcium chloride is essentially constant in metasomatic processes, but that of magnesium chloride may be a sensitive function of reaction progress.[4] Because the concentration of aqueous silica in fluids coexisting with calcium magnesium silicates is also high compared to that of magnesium at

[4] This conclusion follows in part from the observation that a relatively small change in a large concentration has an insignificant effect on the magnitude of the concentration, which is not true of the same change in a small concentration.

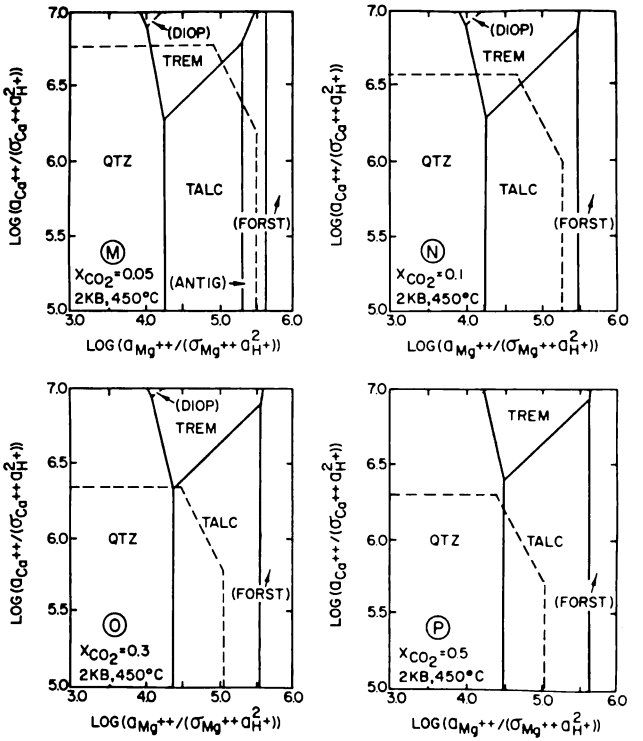

Fig. 8. Logarithmic activity diagrams for the system CaO–MgO–SiO_2–HCl–CO_2–H_2O at 2 kb and 450°C for X_{CO_2} = 0.05, 0.10, 0.30, and 0.50 (see caption of fig. 5).

high temperatures and pressures (see below), silica would be expected to exhibit behavior similar to calcium. However, in certain cases (such as fluids coexisting with dolomite, tremolite, and forsterite, or dolomite, tremolite, and talc (figs. 5-8)), substantial mass transfer of magnesium as well as silica and calcium may occur. The latter observation is consistent with the relative mass transfer of calcium, magnesium, and silica accompanying formation of metasomatic veins in Alpine dolomites (Trommsdorff, 1966a; Bucher, ms; Frisch and Helgeson, 1978), as well as that deduced from experimental observations (Hemley and others, 1977a and b). Consequently, in addition to temperature, pressure, and X_{CO_2}, log $(a_{Ca^{++}}/(\sigma_{Ca^{++}}\, a_{H^+}{}^2))$ and log $(a_{SiO_{2(aq)}}/\sigma_{SiO_{2(aq)}})$ are particularly appropriate descriptive variables for interpreting the consequences of equilibrium and mass transfer in the system CaO–MgO–SiO_2–HCl–CO_2–H_2O. Four diagrams cast in terms of the latter two variables are shown in figure 9, where it can be seen that a large stability field of talc separates those of magnesite and tremolite. Note that dolomite coexists with talc over an increasingly larger range of log $(a_{Ca^{++}}/(\sigma_{Ca^{++}}\, a_{H^+}{}^2))$ and log $(a_{SiO_{2(aq)}}/\sigma_{SiO_{2(aq)}})$ as X_{CO_2} increases to 0.4, but then the range decreases with further increase in X_{CO_2}. In contrast, log $(a_{Ca^{++}}/\sigma_{Ca^{++}}\, a_{H^+}{}^2))$ for dolo-

mite coexisting with tremolite first decreases and then increases with increasing X_{CO_2}, owing to truncation of the stability field boundary by calcite saturation.

Correlation of activity and temperature–X_{CO_2} diagrams.—Phase relations in the system CaO–MgO–SiO_2–CO_2–H_2O at $P_{total} = P_{fluid} = 2$ kb are depicted in terms of temperature and X_{CO_2} in figures 10 and 11, which were generated from thermodynamic data and equations summarized by Helgeson and others (1978). Figure 11 represents an enlargement of the hatched area of figure 10. The circled letters in both figures correspond to those in figures 3 and 5 through 8, in which multivariant phase equilibria are depicted in terms of mineral compositions and the activities of aqueous species at the various temperature–X_{CO_2} coordinates corresponding to the circled letters in figures 10 and 11.

Univariant reactions limiting the stability of antigorite ($Mg_{48}Si_{34}O_{85}(OH)_{62}$) are numbered 1 through 5 in figure 10, where it can be deduced that antigorite is compatible with CO_2–H_2O fluids at 2 kb only at temperatures $\leqslant$475°C and $X_{CO_2} \leqslant 0.14$. The configurations of curves 1 through 5 in figure 10 are identical to those of the corresponding curves generated

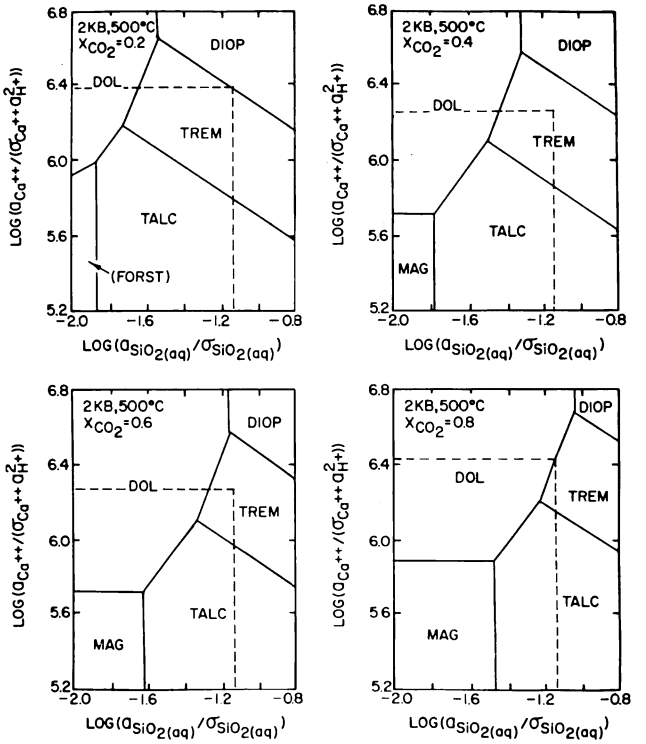

Fig. 9. Logarithmic activity diagrams for the system CaO–MgO–SiO_2–HCl–CO_2–H_2O at 2 kb and 500°C for X_{CO_2} = 0.2, 0.4, 0.6, and 0.8. The dashed lines correspond to saturation in the fluid phase with respect to calcite (horizontal dashed lines) and quartz (vertical dashed lines).

by Trommsdorff and Evans (1977), who give 520°C and $X_{CO_2} = 0.20$ for these limits.

It has already been demonstrated (Helgeson and others, 1978) that the phase relations shown in figures 10 and 11 are in close agreement with the bulk of the experimental data reported by Harker and Tuttle (1956), Greenwood (1967), Gordon and Greenwood (1970), Skippen (1971, 1975), and Slaughter, Kerrick, and Wall (1975). However, figures 10 and 11 are not compatible with certain extrapolations made in these experimental studies, especially at low values of X_{CO_2}. In general, the curves shown in figures 10 and 11 are ~10°C higher at a given X_{CO_2} than those generated by Skippen (1975) and Slaughter, Kerrick, and Wall (1975) from extrapolation of their experimental data. The discrepancies apparently arise from differences in the fugacity coefficients of CO_2 and H_2O employed in the present study and those used by Skippen and Slaughter, Kerrick, and Wall.

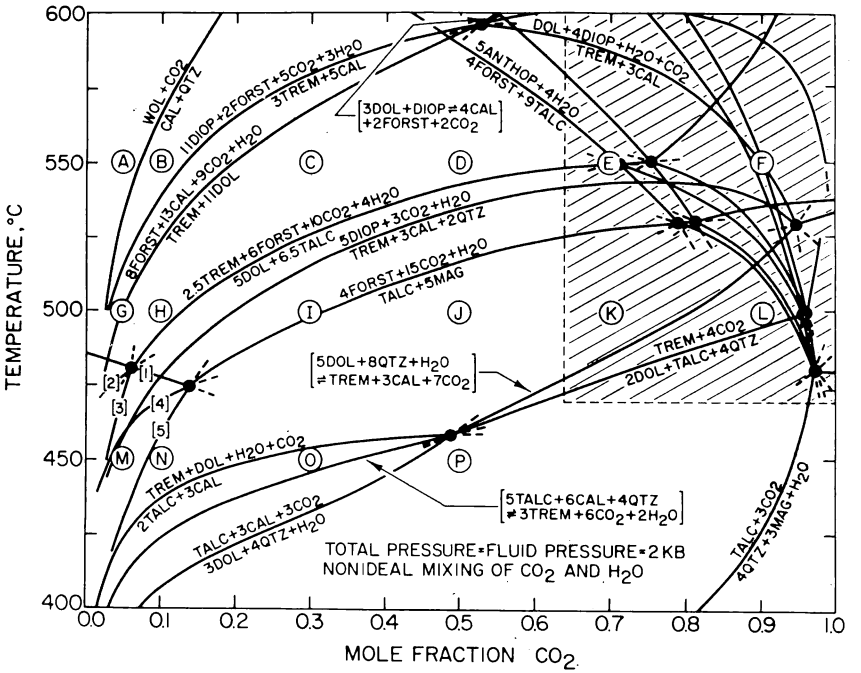

Fig. 10. Temperature–X_{CO_2} diagram for the system CaO–MgO–SiO_2–HCl–CO_2–H_2O generated from thermodynamic calculations (see text). The circled letters indicate mineral assemblages and positions of logarithmic activity diagrams shown in figures 3 and 5 through 8. The numbered curves represent the following reactions involving antigorite ($Mg_{48}Si_{34}O_{85}(OH)_{62}$).

(1) antig $\rightleftharpoons$ 18 forst + 4 talc + 27 H_2O
(2) 40 dol + 13 antig $\rightleftharpoons$ 20 trem + 282 forst + 383 H_2O + 80 CO_2
(3) 47 talc + 30 dol + 30 H_2O $\rightleftharpoons$ 15 trem + 2 antig + 60 CO_2
(4) 20 mag + antig $\rightleftharpoons$ 34 forst + 31 H_2O + 20 CO_2
(5) 17 talc + 45 mag + 45 H_2O $\rightleftharpoons$ 2 antig + 45 CO_2

It can be seen in figures 10 and 11 that 8 invariant points and a myriad of univariant reactions occur among MgO-rich mineral assemblages at 2 kb and high values of X_{CO_2}. Much of the complexity in the phase relations in figure 11 arises from the appearance of anthophyllite and enstatite as stable phases at high X_{CO_2}. Note that anthophyllite is not stable at temperatures below ~480°C, but as temperature increases above ~480°C, anthophyllite becomes stable at increasingly lower values of X_{CO_2}. The stability of anthophyllite in the presence of dolomite is limited to $X_{CO_2} > 0.71$ and temperatures between 500° and 550°C. Chrysotile, which is apparently metastable (Helgeson and others, 1978) and occurs at 2 kb and temperatures <400°C only in H_2O-rich environments, was omitted from figure 10.

Triple points on the activity diagrams shown in figures 5 through 8 correspond to divariant assemblages on the temperature–X_{CO_2} diagrams in figures 10 and 11. The relation of these various diagrams to each other can be assessed with the aid of figure 12, where equilibrium among cal-

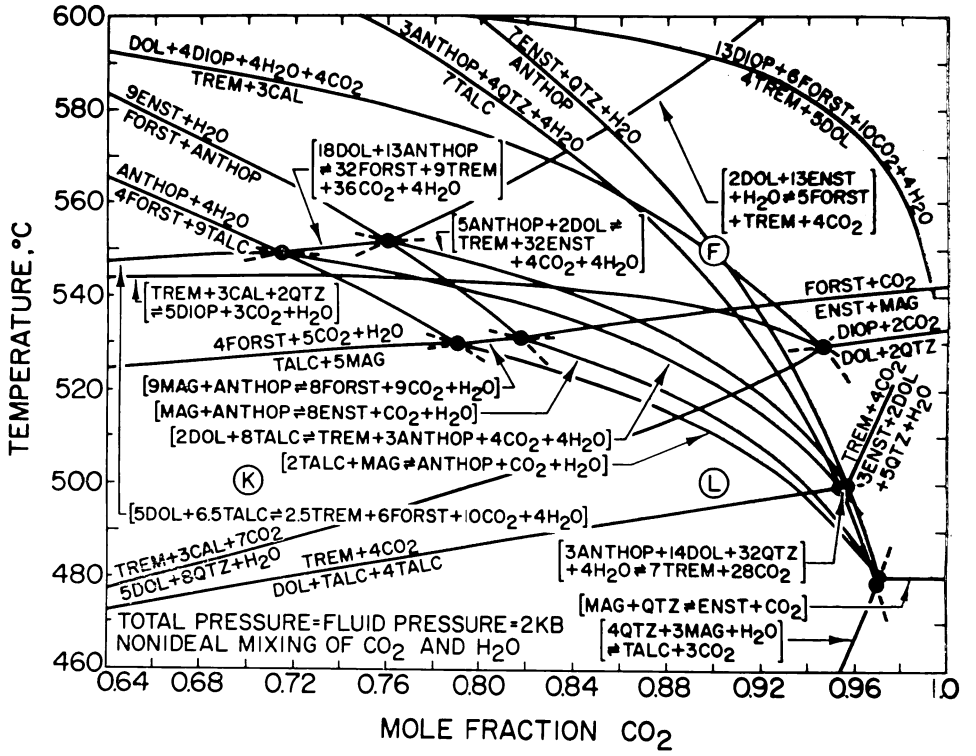

Fig. 11. Enlargement of the CO_2-rich portion of the temperature–X_{CO_2} diagram shown in figure 10. Note that the two invariant points corresponding to the coexistence of magnesite, anthophyllite, quartz, talc, and fluid, and magnesite, anthophyllite, quartz, enstatite, and fluid are nearly coincident on the diagram.

cite, tremolite, dolomite, quartz, and a fluid phase at 2 kb is depicted as a function of temperature, X_{CO_2}, and log $(a_{Mg^{++}}/(\sigma_{Mg^{++}}\ a_{H^+}{}^2))$. The three surfaces labeled CBLD, ACBEF, and AGBN correspond, respectively, to the coexistence of tremolite, dolomite, calcite, and fluid; tremolite, calcite, quartz, and fluid; and calcite, quartz, dolomite, and fluid. Note that the intersection of these surfaces along AB, which represents the coexistence of all five phases, appears as a projection along A′B′ on the front (temperature–X_{CO_2}) face of the block diagram. Note also that surface ACBEF intersects surfaces CBLD and AGBN at higher values of log $(a_{Mg^{++}}/(\sigma_{Mg^{++}}\ a_{H^+}{}^2))$ with both increasing and decreasing X_{CO_2} from $X_{CO_2} = 0.5$.

The phase relations illustrated in three-dimensional space in figure 12 can be depicted in terms of temperature–log $(a_i/(\sigma_i\ a_{H^+}{}^{z_i}))$ and X_{CO_2}–log $(a_i/(\sigma_i\ a_{H^+}{}^{z_i}))$ by taking sections of the block diagram in the planes of MHI and JKL, respectively. Diagrams of this kind afford insight into the sensitivity of various equilibria to relative changes in temperature, X_{CO_2}, and the concentrations of electrolytes in the fluid phase.

Temperature-activity diagrams.—It can be seen in figure 13 that the fluid phase coexisting with the majority of the mineral assemblages shown in the figure at 2 kb, $X_{CO_2} = 0.3$, and temperatures between 400° and 600°C exhibit a remarkably narrow range (3.4–4.8) of log $(a_{Mg^{++}}/(\sigma_{Mg^{++}}\ a_{H^+}{}^2))$. Note also that under these conditions, coexisting calcite and dolomite requires $4.23 < \log (a_{Mg^{++}}/(\sigma_{Mg^{++}}\ a_{H^+}{}^2)) < 4.48$.

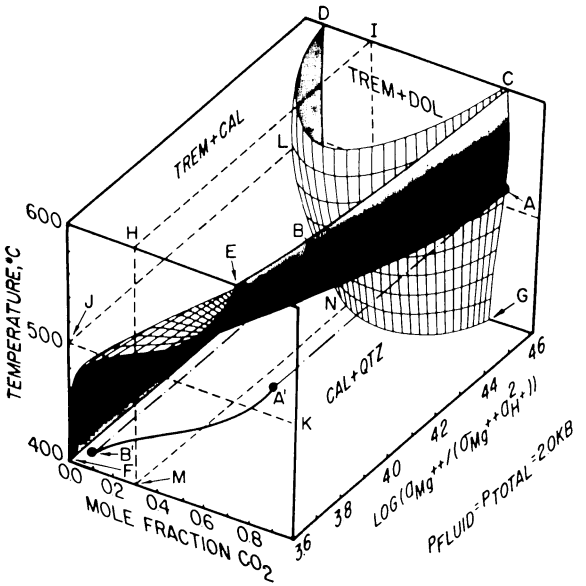

Fig. 12. Phase relations among tremolite, dolomite, calcite, quartz, and a fluid phase as a function of temperature, X_{CO_2}, and log $(a_{Mg^{++}}/(\sigma_{Mg^{++}}\ a_{H^+}{}^2))$ at 2 kb (see text).

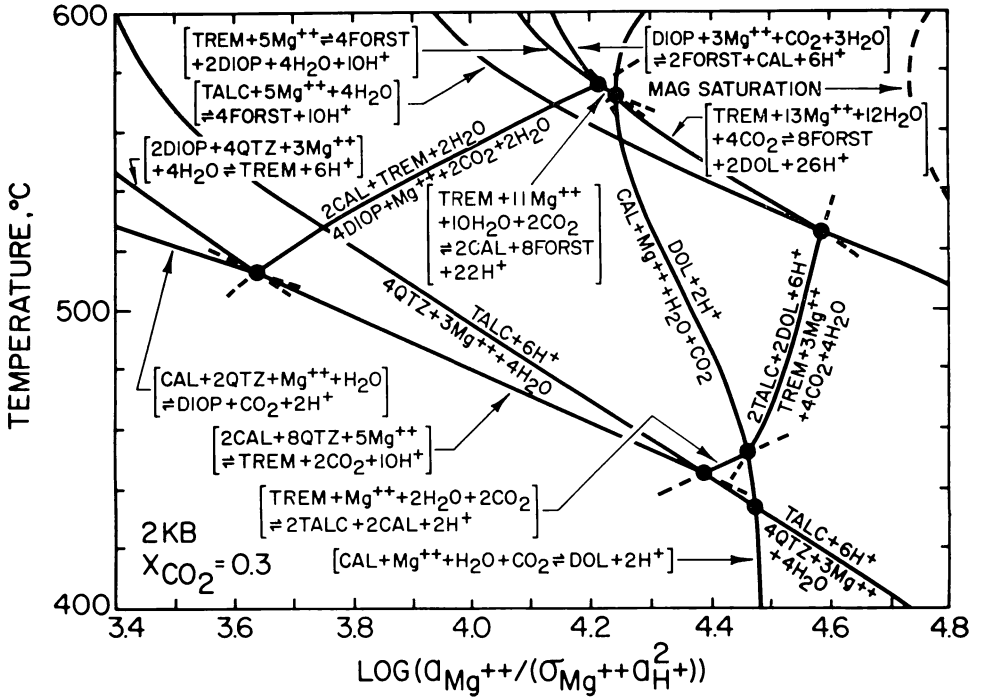

Fig. 13. Phase relations in the system CaO–MgO–SiO_2–HCl–CO_2–H_2O as a function of temperature and log $(a_{Mg^{++}}/(\sigma_{Mg^{++}}\, a_{H^+}{}^2))$ at 2 kb and $X_{CO_2} = 0.3$.

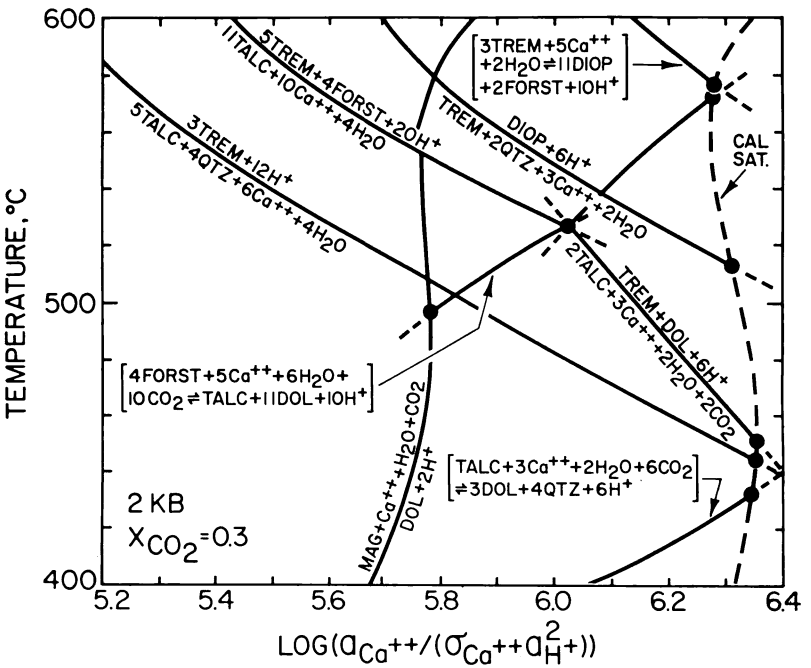

Fig. 14. Phase relations in the system CaO–MgO–SiO_2–HCl–CO_2–H_2O as a function of temperature and log $(a_{Ca^{++}}/(\sigma_{Ca^{++}}\, a_{H^+}{}^2))$ at 2 kb and $X_{CO_2} = 0.3$.

The slopes of the curves shown in figures 13 and 14 are consistent with

$$\left(\frac{\partial T}{\partial \log (a_{Mg^{++}}/(\sigma_{Mg^{++}}\, a_{H^+}{}^2))}\right)_{P,X_{CO_2}} = \frac{2.303\, \hat{n}_{Mg^{++},r}\, RT^2}{\Delta H^\circ_r} \quad (23)$$

and

$$\left(\frac{\partial T}{\partial \log (a_{Ca^{++}}/(\sigma_{Ca^{++}}\, a_{H^+}{}^2))}\right)_{P,X_{CO_2}} = \frac{2.303\, \hat{n}_{Ca^{++},r}\, RT^2}{\Delta H^\circ_r} \quad (24)$$

where $\hat{n}_{Mg^{++},r}$ and $\hat{n}_{Ca^{++},r}$ refer to the reaction coefficients of Mg^{++} and Ca^{++} in the rth reaction (which are positive for products and negative for reactants), and ΔH°_r stands for the standard molal enthalpy of the reaction. Because ΔH°_r is positive for most of the reactions in figures 13 and 14, the slopes of the curves representing these reactions are negative. However, in a few cases (such as diopside, calcite, and tremolite coexisting with a fluid phase), increasing temperature is accompanied by increasing log $(a_{Mg^{++}}/(\sigma_{Mg^{++}}\, a_{H^+}{}^2))$. Note in figure 14 that the presence of calcite in calc–silicate assemblages is restricted to $6.27 < \log (a_{Ca^{++}}/(\sigma_{Ca^{++}}\, a_{H^+}{}^2)) < 6.35$. It should be emphasized that at 2 kb talc coexists with quartz at lower values of $a_{SiO_{2(aq)}}/\sigma_{SiO_{2(aq)}}$ at 400°C than those corresponding to the coexistence of talc and forsterite at 600°C (fig. 15).

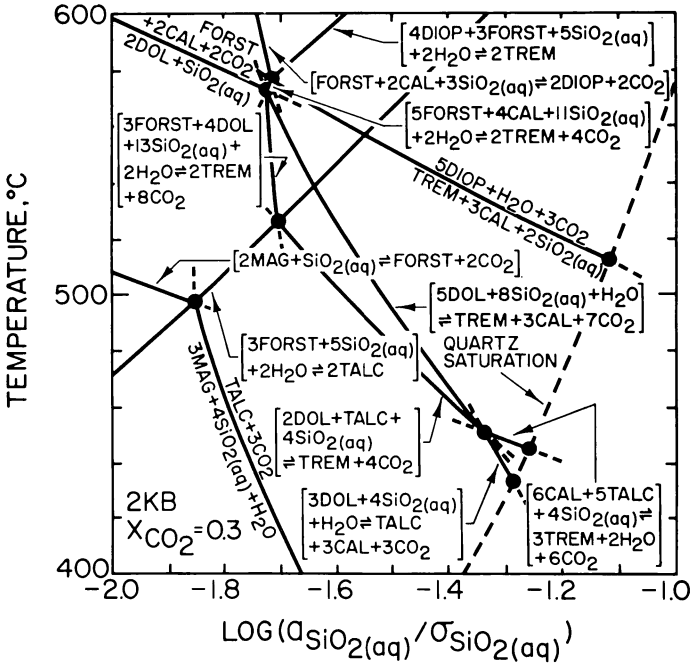

Fig. 15. Phase relations in the system CaO–MgO–SiO_2–HCl–CO_2–H_2O as a function of temperature and log $(a_{SiO_{2(aq)}}/\sigma_{SiO_{2(aq)}})$ at 2 kb and $X_{CO_2} = 0.3$.

X_{CO_2}–activity diagrams.—Phase relations in the system CaO–MgO–SiO_2–HCl–CO_2–H_2O at 2 kb and 450°, 500°, and 550°C are shown in figures 16 through 19 in terms of X_{CO_2} and log $(a_{Mg^{++}}/(\sigma_{Mg^{++}}\, a_{H^+}{}^2))$ or log $(a_{Ca^{++}}/(\sigma_{Ca^{++}}\, a_{H^+}{}^2))$. The configurations of the curves in these figures are similar to those of corresponding curves in temperature–X_{CO_2} diagrams (figs. 10 and 11). The slopes of the curves in figures 16 through 19 can be expressed as

$$\left(\frac{\partial \log (a_i/(\sigma_i\, a_{H^+}{}^{Z_i}))}{\partial X_{CO_2}}\right)_{P,T} = -\frac{1}{2.303\,\hat{n}_{i,r}}\left(\frac{\hat{n}_{CO_2,r}}{X_{CO_2}} - \frac{\hat{n}_{H_2O,r}}{X_{H_2O}}\right)$$

$$-\frac{1}{\hat{n}_{i,r}}\left(\hat{n}_{CO_2,r}\left(\frac{\partial \log \chi_{CO_2}}{\partial X_{CO_2}}\right)_{P,T} + \hat{n}_{H_2O,r}\left(\frac{\partial \log \chi_{H_2O}}{\partial X_{CO_2}}\right)_{P,T}\right) \quad (25)$$

which is similar to the analogous expression derived by Greenwood (1967) for $(\partial T/\partial X_{CO_2})_P$. It follows from eq (25) that for reactions in which $\hat{n}_{CO_2,r}$ and $\hat{n}_{H_2O,r}$ have the same sign, the curves in figures 16 through 19 exhibit extrema, but for those in which $\hat{n}_{CO_2,r}$ and $\hat{n}_{H_2O,r}$ are of opposite sign, the curves are sigmoid. In both cases, departures from symmetry are

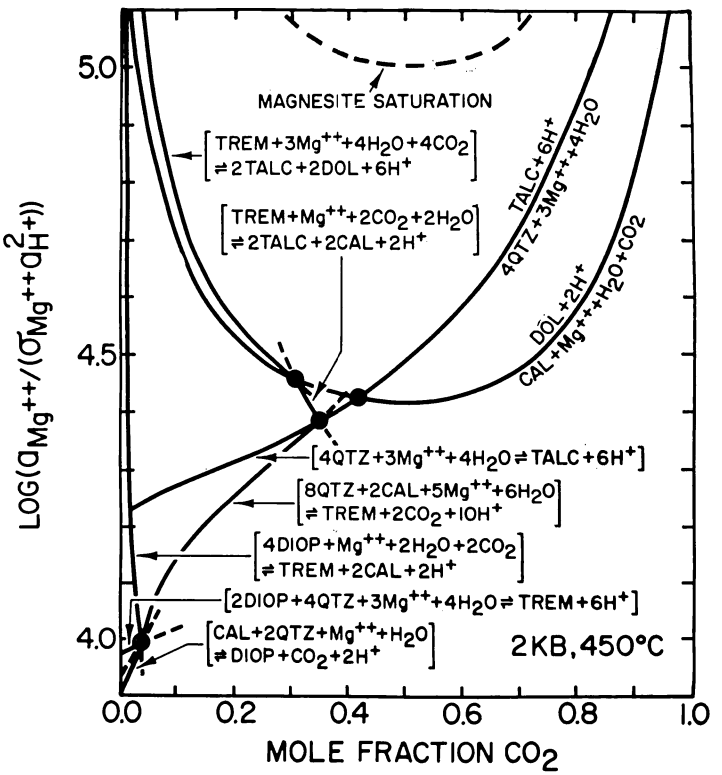

Fig. 16. Phase relations in the system CaO–MgO–SiO_2–HCl–CO_2–H_2O as a function of log $(a_{Mg^{++}}/(\sigma_{Mg^{++}}\, a_{H^+}{}^2))$ and X_{CO_2} at 2 kb and 450°C.

caused by differences in $\hat{n}_{CO_2,r}$ and $\hat{n}_{H_2O,r}$ together with nonideal mixing of CO_2 and H_2O.

It can be deduced by comparison of figures 13 and 16 through 18 that log $(a_{Mg^{++}}/(\sigma_{Mg^{++}}\, a_{H^+}{}^2))$ in fluids coexisting with a given mineral assemblage shown in the figures at 2 kb and 450° to 550°C exhibits a wider range as a function of X_{CO_2} at constant temperature than it does as a function of temperature at constant X_{CO_2}. Note also in figure 19 that dolomite can exist over a range of log $(a_{Ca^{++}}/(\sigma_{Ca^{++}}\, a_{H^+}{}^2))$ spanning 0.5 log units at most values of X_{CO_2}.

Diagrams for systems with an ubiquitous solid phase.—Phase relations among a fluid phase and minerals in the system CaO–MgO–SiO_2–CO_2–H_2O in the presence of quartz are depicted in figures 20 through 22 as a function of log $(a_{Mg^{++}}/(\sigma_{Mg^{++}}\, a_{H^+}{}^2))$, log $(a_{Ca^{++}}/(\sigma_{Ca^{++}}\, a_{H^+}{}^2))$, and log a_{H_2O} at 2 kb and 450°, 500°, and 550°C. In contrast, calcite is specified as an ubiquitous phase in figure 23, where the descriptive variables are log $(a_{SiO_{2(aq)}}/\sigma_{SiO_{2(aq)}})$ and log a_{H_2O}.

Because the presence of quartz fixes the activity of $SiO_{2(aq)}$ at constant pressure and temperature, talc is stable only along saturation lines in figures 20A, 21A, and 22A, which define upper limits of log $(a_{Mg^{++}}/(\sigma_{Mg^{++}}\, a_{H^+}{}^2))$ and log $(a_{Ca^{++}}/(\sigma_{Ca^{++}}\, a_{H^+}{}^2))$ for the coexistence of quartz, talc,

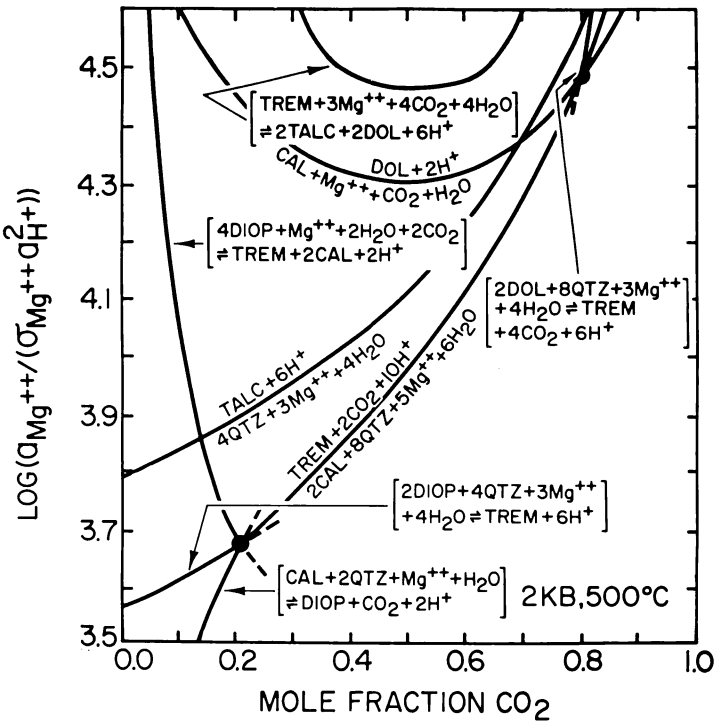

Fig. 17. Phase relations in the system CaO–MgO–SiO_2–HCl–CO_2–H_2O as a function of log $(a_{Mg^{++}}/(\sigma_{Mg^{++}}\, a_{H^+}{}^2))$ and X_{CO_2} at 2 kb and 500°C.

and a fluid phase. As a consequence, quartz, talc, and tremolite may coexist with a fluid phase at lower values of log a_{H_2O} as temperature increases at constant pressure. Note that the stability field of dolomite + quartz decreases in size considerably with increasing temperature, but that of diopside + quartz increases.

It can be seen in figure 23 that quartz saturation restricts severely the range of composition of fluids coexisting with either talc or tremolite and calcite. With increasing temperature the stability fields of diopside + calcite and tremolite + calcite increase at the expense of that for talc + calcite. Note that in contrast to fluids coexisting with tremolite, dolo-

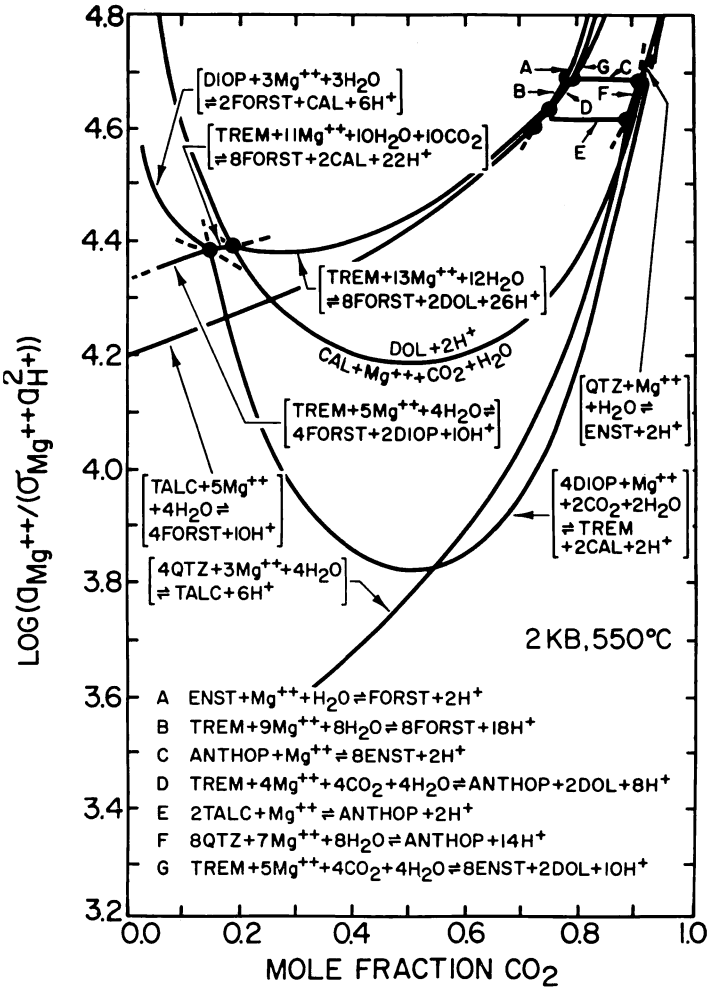

Fig. 18. Phase relations in the system CaO–MgO–SiO_2–HCl–CO_2–H_2O as a function of log ($a_{Mg^{++}}/(\sigma_{Mg^{++}} a_{H^+}^2)$) and X_{CO_2} at 2 kb and 550°C.

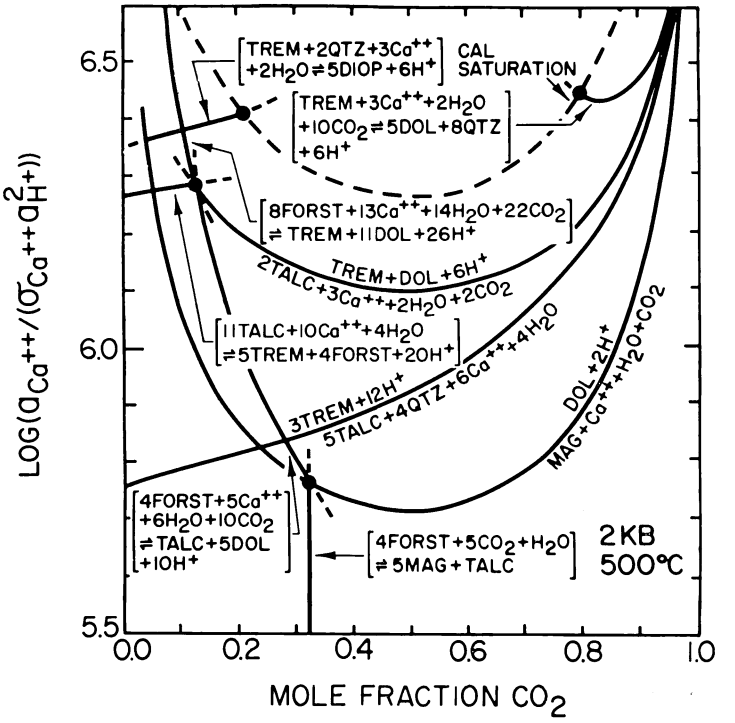

Fig. 19. Phase relations in the system CaO–MgO–SiO_2–HCl–CO_2–H_2O as a function of log $(a_{Ca^{++}}/(\sigma_{Ca^{++}}\, a_{H^+}{}^2))$ and X_{CO_2} at 2 kb and 500°C.

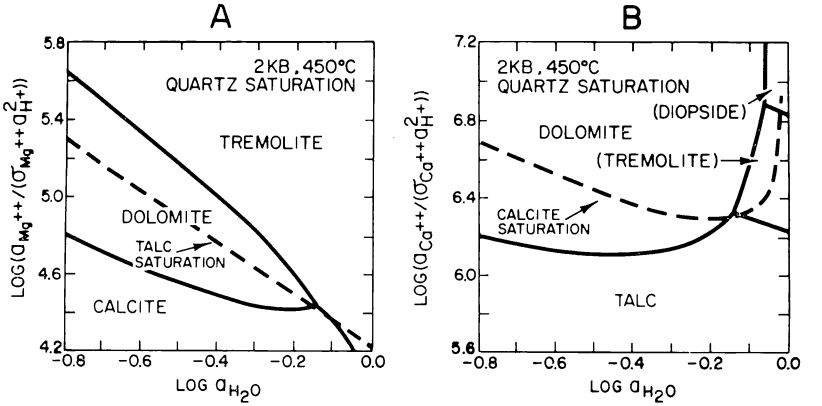

Fig. 20. Phase relations in the system CaO–MgO–SiO_2–HCl–CO_2–H_2O in the presence of quartz as a function of log $(a_{Mg^{++}}/(\sigma_{Mg^{++}}\, a_{H^+}{}^2))$, log $(a_{Ca^{++}}/(\sigma_{Ca^{++}}\, a_{H^+}{}^2))$, and log a_{H_2O} at 2 kb and 450°C.

mite, quartz, and calcite, those in equilibrium with diopside, tremolite, quartz, and calcite are H_2O-rich.

CONCLUDING REMARKS

The activity diagrams presented in the foregoing pages represent relatively few of the many combinations of descriptive variables that can be used to describe and interpret metasomatic phase equilibria at high pressures and temperatures. Multiple generation of these diagrams with the aid of remote interactive numerical and graphic computer techniques facilitates rapid and comprehensive thermodynamic analysis of complex phase relations in multicomponent systems. As more and better data become available from which to calculate dissociation constants, activity coefficients, and values of σ_i, the utility of activity diagrams applied to metamorphic systems will increase. However, even in the present state of knowledge they afford a comprehensive frame of reference for guiding experimental studies and mapping multivariant phase relations observed in the field on chemical potential (activity) coordinates. Because these coordinates can be correlated with their geographic counterparts, the approach enhances considerably detection of spatial and temporal trends in temperature, pressure, and fluid composition. In addition, it affords a means to discriminate quantitatively among causal and dependent variables in geochemical processes, which will be the subject of a later communication in this series.

ACKNOWLEDGMENTS

The research reported in this paper represents the second part of the senior author's Ph.D. dissertation at the University of California, Berkeley. We are indebted to Per Aagaard, Dennis Bird, George Flowers, Connie Frisch, William McKenzie, Mike Lee, Joachim Hampel, Debbie Aoki, Terri Brooks, Barbara Rosenbaum, Joan Bossart, and others among our friends and colleagues at Berkeley for helpful suggestions, assistance, and

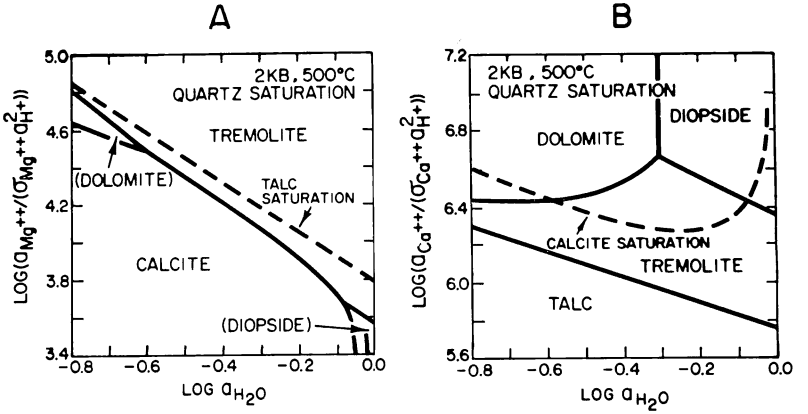

Fig. 21. Phase relations in the system CaO–MgO–SiO_2–HCl–CO_2–H_2O in the presence of quartz as a function of log $(a_{Mg^{++}}/(\sigma_{Mg^{++}}\ a_{H^+}{}^2))$, log $(a_{Ca^{++}}/(\sigma_{Ca^{++}}\ a_{H^+}{}^2))$, and log a_{H_2O} at 2 kb and 500°C.

encouragement during the course of this research. Thanks are also due Volkmar Trommsdorff and his students for their hospitality and stimulating discussions during a 9-month stay by one of us (J.V.W.) at the Eigennössische Technische Hochschule in Zurich. Various aspects of this project were supported by the National Science Foundation (NSF grants EAR 74-14280 and EAR 77-14492), the donors of the Petroleum Research Fund administered by the American Chemical Society (PRF grants 5356 AC2 and 8927 AC2C), the Miller Institute and Committee on Research at the University of California, Berkeley, and the Division of Physical Research of the U.S. Energy Research and Development Administration (ERDA Contract Nos. 7405-ENG-48 and UCB-ENG-4288). Finally we would like to express our appreciation to L. Brewer, I. S. E. Carmichael,

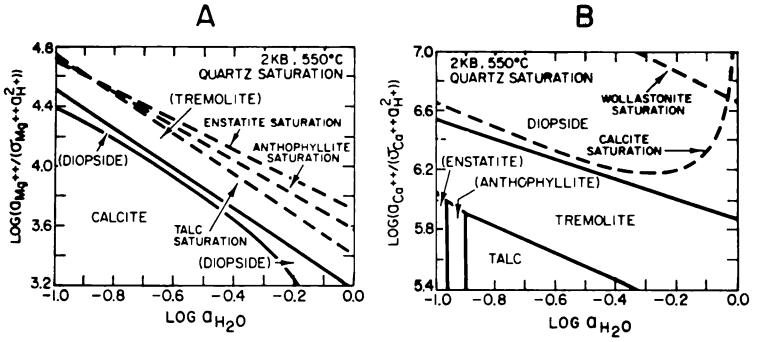

Fig. 22. Phase relations in the system CaO–MgO–SiO_2–HCl–CO_2–H_2O in the presence of quartz as a function of log $(a_{Mg^{++}}/(\sigma_{Mg^{++}}\ a_{H^+}{}^2))$, log $(a_{Ca^{++}}/(\sigma_{Ca^{++}}\ a_{H^+}{}^2))$, and log a_{H_2O} at 2 kb and 550°C.

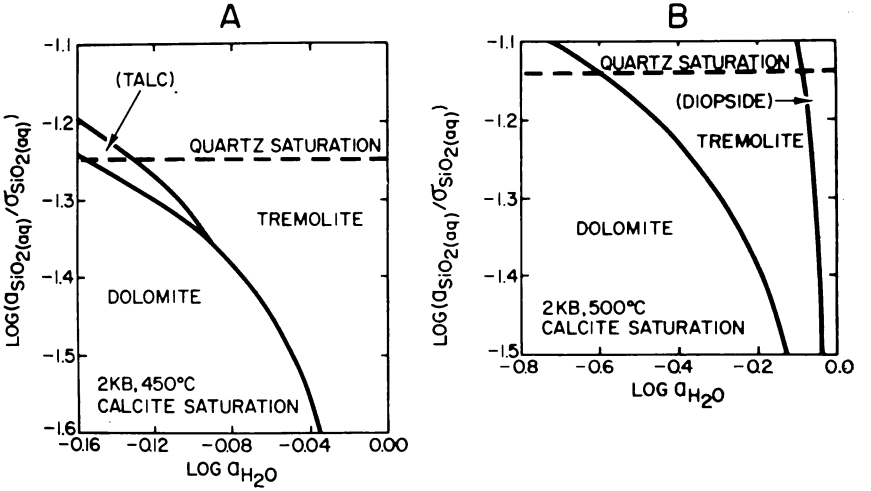

Fig. 23. Phase relations in the system CaO–MgO–SiO_2–HCl–CO_2–H_2O in the presence of calcite as a function of log $(a_{SiO_2(aq)}/\sigma_{SiO_2(aq)})$ and log a_{H_2O} at 2 kb and 450° and 500°C.

G. C. Flowers, J. V. Chernosky, J. J. Hemley, P. M. Orville, G. M. Anderson, and J. D. Frantz for critical reviews of the manuscript and helpful suggestions for improvement.

References

Althaus, E., and Johannes, W., 1969, Experimental metamorphism of NaCl-bearing aqueous solutions by reaction with silicates: Am. Jour Sci., v. 267, p. 87-98.

Anderson, G. M., and Burnham, C. W., 1967, Reactions of quartz and corundum with aqueous chloride and hydroxide solutions at high temperatures and pressures: Am. Jour. Sci., v. 265, p. 12-27.

Barnes, H. L., and Ernst, W. G., 1963, Ideality and ionization in hydrothermal fluids: The system MgO–H_2O–NaOH: Am. Jour. Sci., v. 261, p. 129-150.

Bockris, J. O'M., 1949, Ionic Solvation: Quart. Rev. (London), v. 3, p. 173-180.

Bockris, J. O'M., Saluja, P. P. S., and Madan, G., 1970, The study of ionic solvation: Washington, D.C., U.S. Dept. Interior, Office of Saline Water, Research, and Devel. Prog. Rept. 569, 155 p.

Bucher, K. E., ms, 1977, Hochmetamorphe Dolomitmarmore und zonierte metasomatische Adern im obern val Sissone (Provinz Sondrio, Norditalien): Ph.D. dissert., Eidgenössischen Tech. Hochschule, Zürich, 249 p.

Carmichael, D. M., 1969, On the mechanism of prograde metamorphic reactions in quartz-bearing pelitic rocks: Contr. Mineralogy Petrology, v. 20, p. 244-267.

Carswell, D. A., Curtis, C. D., and Kanaris-Sotiriou, R., 1974, Vein metasomatism in peridotite at Kalskaret near Tafjord, South Norway: Jour. Petrology, v. 15, p. 383-402.

Cermignani, C., and Anderson, G. M., 1973, Origin of a diopside-tremolite assemblage near Tweed, Ontario: Canadian Jour. Earth Sci., v. 10, p. 84-90.

Chou, I-Ming, and Eugster, H. P., 1977, Solubility of magnetite in supercritical chloride solutions: Am. Jour. Sci., v. 277, p. 1296-1314.

Chou, I-Ming, and Frantz, J. D., 1977, Recalibration of Ag + AgCl acid buffer at elevated pressures and temperatures: Am. Jour. Sci., v. 277, p. 1067-1072.

Conway, B. E., 1966, Electrolyte solutions: Solvation and structural aspects: Ann. Rev. Phys. Chemistry, v. 17, p. 481-528.

Delany, J. M., and Helgeson, H. C., 1978, Calculation of the thermodynamic consequences of dehydration in subducting oceanic crust to 100 kb and >800°C: Am. Jour. Sci., v. 278, p. 638-686.

Desnoyers, J. E., and Jolicoeur, C., 1969, Hydration effects and thermodynamic properties of ions, *in* Bockris, J. O'M., and Conway, B. E., eds., Modern aspects of electrochemistry, no. 5: New York, Plenum Press, p. 1-89.

Ellis, A. J., 1963, The solubility of calcite in sodium chloride solutions at high temperatures: Am. Jour. Sci., v. 261, p. 49-60.

———— 1968, Natural hydrothermal systems and experimental hot-water/rock interaction: Reactions with NaCl solutions and trace metal extraction: Geochim. et Cosmochim. Acta, v. 32, p. 1356-1363.

———— 1969, Present day hydrothermal systems and mineral deposition: Commonwealth Mining Metallurgical Cong., 9th, London, Proc., p. 12-27.

Eugster, H. P., 1970, Thermal and ionic equilibria among muscovite, K-feldspar and aluminosilicate assemblages: Fortschr. Mineralogie, v. 47, p. 106-123.

Evans, B. W., 1965, Application of a reaction-rate method of the breakdown equilibria of muscovite and muscovite plus quartz: Am. Jour. Sci., v. 263, p. 647-667.

Evans, B. W., and Trommsdorff, V., 1974, Stability of Enstatite + Talc, and CO_2-metamorphism of metaperidotite, Val d'Efra, Lepontine Alps: Am. Jour. Sci., v. 274, p. 274-296.

Flowers, G. C., 1979, Correction of Holloway's (1977) adaptation of the modified Redlich-Kwong equation of state for calculation of the fugacities of molecular species in supercritical fluids of geologic interest: Contr. Mineralogy Petrology, v. 69, p. 315-318.

Frank, E. U., 1980, Survey of selected non-thermodynamic properties and chemical phenomena of fluids and fluid mixtures, *in* Wickman, F., and Rickard, D., eds., Nobel Symposium on Chemistry and Geochemistry of Solutions at High Temperatures and Pressures: Stockholm, Royal Swedish Acad. Sci., in press.

Frank, H. S., 1966, Solvent models and the interpretation of ionization and solvation phenomena, *in* Conway, B. E., and Barradas, R. G., eds., Chemical physics of ionic solutions: New York, John Wiley & Sons, Inc., p. 53-66.

Frantz, J. D., and Eugster, H. P., 1973, Acid-base buffers: Use of Ag + AgCl in the experimental control of solution equilibria at elevated temperatures and pressures: Am. Jour. Sci., v. 273, p. 268-286.

Frantz, J. D., and Popp, R. K., 1977, Determination of aqueous magnesian speciation in the system: MgO–SiO_2–H_2O–HCl: EOS, Am. Geophys. Union Trans., v. 58, p. 1243.

———— 1979, Mineral-solution equilibria — I. An experimental study of complexing and thermodynamic properties of aqueous $MgCl_2$ in the system MgO–SiO_2–H_2O–HCl: Geochim. et Cosmochim. Acta, v. 43, p. 1223-1239.

Friedman, H. L., and Krishnan, C. V., 1973, Thermodynamics of ionic solvation, *in* Franks, F., ed., Water, v. 3, Aqueous solutions of simple electrolytes: New York, Plenum Press, p. 1-118.

Frisch, C. J., and Helgeson, H. C., 1980, Investigation of metasomatic phase equilibria in dolomites of the Adamello Alps: Am. Jour. Sci., v. 280, in press.

Garrels R. M., 1954, Mineral species as functions of pH and oxidation-reduction potentials, with special reference to the zone of oxidation and secondary enrichment of sulphide ore deposits: Geochim. et Cosmochim. Acta, v. 5, p. 153-168.

Garrels, R. M., and Christ, C. L., 1965, Minerals, solutions and equilibria: San Francisco, Freeman, Cooper and Co., 450 p.

Gehrig, M., Lentz, H., and Franck, E. U., 1979, Thermodynamic properties of water–carbon dioxide–sodium chloride mixtures at high temperatures and pressures, *in* Timmerhaus, K. D., and Barber, M. S., eds., High-Pressure Science and Technology, v. 1, Physical Properties and Material Synthesis: New York, Plenum Press, p. 539-542.

Glassley, W. E., 1975, High grade regional metamorphism of some carbonate bodies: Significance for the orthopyroxene isograd: Am. Jour. Sci., v. 275, p. 1133-1163.

Goldsmith, J. R., and Newton, R. C., 1969, P–T–X relations in the system $CaCO_3$–$MgCO_3$ at high temperatures and pressures: Am. Jour. Sci., v. 267-A, p. 160-190.

Gordon, T. M., 1971, Some observations on the formation of wollastonite from calcite and quartz: Canadian Jour. Earth Sci., v. 8, p. 844-861.

Gordon, T. M., and Greenwood, H. J., 1970, The reaction: dolomite + quartz + water = talc + calcite + carbon dioxide: Am. Jour. Sci., v. 268, p. 225-242.

Graf, D. L., and Goldsmith, J. R., 1958, The solid solubility of $MgCO_3$ in $CaCO_3$: A revision: Geochim. et Cosmochim. Acta, v. 13, p. 218-219.

Greenwood, H. J., 1976, Wollastonite: stability in H_2O–CO_2 mixtures and occurrence in a contact-metamorphic aureole near Salmo, British Columbia, Canada: Am. Mineralogist, v. 52, p. 1669-1680.

Gunter, W. D., and Eugster, H. P., 1978, Wollastonite solubility and free energy of supercritical aqueous $CaCl_2$: Contr. Mineralogy Petrology, v. 66, p. 271-281.

Harker, R. I., and Tuttle, O. F., 1956, Experimental data on the P_{CO_2}–T curve for the reaction: calcite + quartz = wollastonite + CO_2: Am. Jour. Sci., v. 254, p. 239-256.

Helgeson, H. C., 1964, Complexing and hydrothermal ore deposition: New York, Pergamon Press, 128 p.

———— 1967a, Thermodynamics of complex dissociation in aqueous solution at elevated temperatures: Jour. Phys. Chemistry, v. 71, p. 3121-3136.

———— 1967b, Solution chemistry and metamorphism, *in* Abelson, P. H., ed., Researches in Geochemistry, v. 2: New York, John Wiley & Sons, p. 362-404.

———— 1968, Evaluation of irreversible reactions in geochemical processes involving minerals and aqueous solutions. I. Thermodynamic relations: Geochim. et Cosmochim. Acta, v. 32, p. 853-877.

———— 1969, Thermodynamics of hydrothermal systems at elevated temperatures and pressures: Am. Jour. Sci., v. 267, p. 729-804.

———— 1970a, A chemical and thermodynamic model of ore deposition in hydrothermal systems: Fiftieth Anniversary Symposia: Mineralog. Soc. America Spec. Paper, v. 3, p. 155-186.

———— 1970b, Description and interpretation of phase relations in geochemical processes involving aqueous solutions: Am. Jour. Sci., p. 415-438.

———— 1980, Prediction of the thermodynamic properties of electrolytes at high pressures and temperatures, *in* Wickman, F., and Rickard, D., eds., Nobel Symposium on Chemistry and Geochemistry of Solutions at High Temperatures and Pressures: Stockholm, Royal Swedish Acad. Sci., in press.

Helgeson, H. C., Brown, T. H., and Leeper, R. H., 1969, Handbook of theoretical activity diagrams depicting chemical equilibria in geologic systems involving minerals and an aqueous phase at one atm and 0°-300°C: San Francisco, Freeman, Cooper and Company, 253 p.

Helgeson, H. C., Delany, J. M., Nesbitt, H. W., and Bird, D. K., 1978, Summary and critique of the thermodynamic properties of minerals: Am. Jour. Sci., v. 278A, 229 p.

Helgeson, H. C., Garrels, R. M., and MacKenzie, F. T., 1969, Evaluation of irreversible reactions in geochemical processes involving minerals and aqueous solutions. II. Applications: Geochim. et Cosmochim. Acta, v. 33, p. 455-481.

Helgeson, H. C., and James, W. R., 1968, Activity coefficients in concentrated electrolyte solutions at high temperatures: Am. Chem. Soc., Abs. of Papers, San Francisco: p. 130.

Helgeson, H. C., and Kirkham, D. H., 1974, Theoretical prediction of the thermodynamic behavior of aqueous electrolytes at high pressures and temperatures: I. Summary of the thermodynamic/electrostatic properties of the solvent: Am. Jour. Sci., v. 274, p. 1089-1198.

———— 1976, Theoretical prediction of the thermodynamic behavior of aqueous electrolytes at high pressures and temperatures: III. Equation of state for aqueous species at infinite dilution: Am. Jour. Sci., v. 276, p. 97-240.

Helgeson, H. C., Kirkham, D. H., and Flowers, G. C., in press, Theoretical prediction of the thermodynamic behavior of aqueous electrolytes at high pressures and temperatures: IV: Calculation of activity and osmotic coefficients and apparent molal and standard and relative partial molal properties to 600°C and 5 kb: Am. Jour. Sci., in press.

Helgeson, H. C., and Mackenzie, F. T., 1970, Silicate-sea water equilibria in the ocean system: Deep Sea Research, v. 17, p. 877-892.

Hemley, J. J., 1959, Some mineralogical equilibria in the system K_2O–Al_2O_3–SiO_2–H_2O: Am. Jour. Sci., v. 257, p. 241-270.

———— 1967, Aqueous Na/K rations in the system K_2O–Na_2O–Al_2O_3–SiO_2–H_2O [abs]: Geol. Soc. America Abs. with Programs, p. 94-95.

Hemley, J. J., and Jones, W. R., 1964, Chemical aspects of hydrothermal alteration with emphasis on hydrogen metasomatism: Econ. Geology, v. 59, p. 538-569.

Hemley, J. J., Montoya, J. W., Christ, C. L., and Hostetler, P. B., 1977a, Mineral equilibria in the MgO–SiO_2–H_2O system: I. talc–chrysotile–forsterite–brucite stability relations: Am. Jour. Sci., v. 277, p. 322-351.

Hemley, J. J., Montoya, J. W., Marienko, J. W., and Luce, R. W., 1980, Mineral equilibria in the system Al_2O_3–SiO_2–H_2O and some implications to alteration/mineralization processes: Econ. Geology, v. 75, p. 210-228.

Hemley, J. J., Montoya, J. W., Nigrini, A., and Vincent, H. A., 1971, Some alteration reactions in the system CaO–Al_2O_3–SiO_2–H_2O: Soc. Mining Geology, Japan, Spec. Issue, v. 2, p. 58-63.

Hemley, J. J., Montoya, J. W., Shaw, D. R., and Luce, R. W., 1977b, Mineral equilibria in the MgO–SiO_2–H_2O system: II. Talc–antigorite–forsterite–anthophyllite–enstatite stability relations and some geologic implications in the system: Am. Jour. Sci., v. 277, p. 353-383.

Hepler, L. G., and Woolley, E. M., 1973, Hydration effects and acid-base equilibria, *in* Franks, F., ed., Water, v. 3, Aqueous solutions of simple electrolytes: New York, Plenum Press, p. 145-172.

Hess, P. C., 1966, Phase equilibria of some minerals in the K_2O–Na_2O–Al_2O_3–SiO_2–H_2O system at 25°C and 1 atmosphere: Am. Jour. Sci., v. 264, p. 289-309.

Hewitt, D. A., 1973, The metamorphism of micaceous limestones from south-central Connecticut: Am. Jour. Sci., v. 273-A, p. 22-40.

Holloway, J. R., 1977, Fugacity and activity of molecular species in supercritical fluids, *in* Fraser, D. G., ed., Thermodynamics in Geology: Dordrecht-Holland, D. Reidel, p. 161-181.

Hutcheon, Ian, and Moore, J. M., 1973, The tremolite isograd near Marble Lake, Ontario: Canadian Jour. Earth Sci., v. 10, p. 936-947.

Iiyama, J. T., 1964, Étude des réactions d'échange d'ions Na–K dans la série muscovite–paragonite: Soc. franç. mineralogie cristallographie Bull., v. 87, p. 532-541.

———— 1966, Contribution à l'étude des équilibres sub-solidus du système ternaire orthose–albite–anorthite à l'aide des réactions d'échange d'ions Na–K au contact d'une solution hydrothermale: Soc. franç. mineralogie cristallographie Bull., v. 89, p. 442-454.

———— 1970, Influence de la pression sur la composition de la solution hydrothermal sodi–potassique de diver sels en équilibre avec les feldspaths perthitiques à 600°C. Observation expérimentale: Acad. Sci. Paris Comptes rendus, v. 271, p. 1925-1927.

Joesten, R., 1976, High temperature contact metamorphism of carbonate rocks in a shallow crustal environment, Christmas Mountains, Big Bend region, Texas: Am. Mineralogist, v. 61, p. 776-781.

Journet, G., and Vadon, J., 1955, Acquisitions récentes concernant l'hydration des ions: Soc. chim. France Bull., v. 22, p. 593-607.

Kavanau, J. L., 1964, Water and solute-water interactions: San Francisco, Holden-Day Inc., 101 p.

Kerrick, D. M., 1974, Review of metamorphic mixed-volatile (H_2O–CO_2) equilibria: Am. Mineralogist, v. 59, p. 729-762.

———— 1977, The genesis of zoned skarns in the Sierra Nevada, California: Jour. Petrology, v. 18, p. 144-181.

Kerrick, D. M., Crawford, K. E., and Randazzo, A. F., 1973, Metamorphism of calcareous rocks in three roof pendants in the Sierra Nevada, California: Jour. Petrology, v. 14, p. 303-325.

Kridelbaugh, S. J., 1973, The kinetics of the reaction: calcite + quartz = wollastonite + carbon dioxide at elevated temperatures and pressures: Am. Jour. Sci., v. 273, p. 757-777.

Kwak, T. A. P., 1971a, Justification for both ionic and thermal reactions in Grenville Province pelitic rocks near Sudbury, Ontario, Canada: Canadian Jour. Earth Sci., v. 8, p. 1333-1354.

———— 1971b, The selective replacement of the aluminum silicates by white mica: Contr. Mineralogy Petrology, v. 32, p. 193-210.

Ling, G. N., 1972, Hydration of macromolecules, *in* Horne, R. A., ed., Water and aqueous solutions: New York, Wiley-Interscience, p. 663-700.

McKenzie, W. F., and Helgeson, H. C., 1979, Calculations of the dielectric constant of H_2O and the thermodynamic properties of aqueous species at temperatures to 900°C: Geol. Soc. America Abs. with Programs, v. 11, p. 476.

Melson, W. G., 1966, Phase equilibria in calc–silicate hornfels, Lewis and Clark County, Montana: Am. Mineralogist, v. 51, p. 402-421.

Mercolli, I., ms, 1978, Le fasi fluide associate al metamorfismo delle dolomie silicce del Campolungo (Ticino): Ph.D. dissert., Eidgenössichen Tech. Hochschule, Zürich.

Metz, P., 1967, Experimentalle Bildung von Forsterit und Calcit aus Tremolit und Dolomit: Geochim. et Cosmochim. Acta, v. 31, p. 1517-1532.

———— 1970, Experimentelle Untersuchung der metamorphose von Kieselig dolomitischen Sedimenten: Contr. Mineralogy Petrology, v. 28, p. 221-250.

Metz, P., and Trommsdorff, V., 1968, On phase equilibria in metamorphosed siliceous dolomites: Contr. Mineralogy Petrology, v. 18, p. 305-309.

Metz, P., and Winkler, G. F., 1963, Experimentelle Gesteinmetamorphose — VII. Die Bildung von Talc aus Kieseligen Dolomit: Geochim. et Cosmochim. Acta, v. 27, p. 431-457.

Mikhailov, V. A., and Drakin, S. I., 1960, Mechanism of the solvation of ions: Akad. Nauk SSSR Izv. Sibirsk. Otd., v. 6, p. 44-52.

Montoya, J. W., and Hemley, J. J., 1975, Activity relations and stabilities in alkali feldspar and mica alteration reactions: Econ. Geology, v. 70, p. 577-594.

Moore, J. N., and Kerrick, D. M., 1976, Equilibria in siliceous dolomites of the Alta aureole, Utah: Am. Jour. Sci., v. 276, p. 502-524.

Morgan, B. A., 1975, Mineralogy and origin of skarn in the Mount Morrison pendant, Sierra Nevada, California: Am. Jour. Sci., v. 275, p. 119-142.

Muirhead-Gould, J. S., and Laidler, K. J., 1966, The thermodynamic properties of charge-bearing systems in aqueous solutions: A discontinuous model for octahedral hydration, *in* Conway, B. E., and Barradas, R. G., eds., Chemical physics of ionic solutions: New York, John Wiley & Sons, Inc., p. 75-86.

Newton, R. C., 1966, Some calc–silicate equilibrium relations: Am. Jour. Sci., v. 264, p. 204-222.

Nightingale, E. R., 1966, On the specificity of electrolyte solvation, *in* Conway, B. E., and Barradas, R. G., eds., Chemical physics of ionic solutions: New York, John Wiley & Sons, Inc., p. 87-100.

Novgorodov, P. G., 1975, Quartz solubility in H_2O–CO_2 mixtures at 700°C and pressures of 3 and 5 kbar: Geokhimica, no. 10, p. 1484-1489.

Orville, P. M., 1963, Alkali ion exchange between vapor and feldspar phases: Am. Jour. Sci., v. 261, p. 201-237.

———— 1972, Plagioclase cation exchange equilibria with aqueous chloride solution: Results at 700°C and 2000 bars in the presence of quartz: Am. Jour. Sci., v. 272, p. 234-272.

Poty, B. P., Holland, H. D., and Borcsik, M., 1972, Solution-mineral equilibria in the system MgO–SiO_2–H_2O–$MgCl_2$ at 500°C and 1 kbar: Geochim. et Cosmochim. Acta, v. 36, p. 1101-1113.

Poty, B. P., Stalder, H. A., and Weisbrod, A. M., 1974, Fluid inclusion studies in quartz from fissures of Western and Central Alps: Schweizer. min. pet. Mitt., v. 54, p. 717-752.

Prue, J. E., 1966, Ion association and solvation, *in* Conway, B. E., and Barradas, R. G., eds., Chemical physics of ionic solutions: New York, John Wiley & Sons, Inc., p. 163-174.

Puhan, D., and Hoffer, E., 1973, Phase relations of talc and tremolite in metamorphic calcite–dolomite sediments in the southern portion of the Damara Belt (South West Africa): Contr. Mineralogy Petrology, v. 40, p. 207-214.

Rice, J. M., 1977, Progressive metamorphism of impure dolomitic limestone in the Marysville Aureole, Montana: Am. Jour. Sci., v. 277, p. 1-24.

Samoilov, O. Y., 1957, Structure of aqueous electrolyte solutions and the hydration of ions [translated by D. J. G. Ives]: Faraday Soc. Discussions, v. 24, 141 p.

———— 1972, Residence times of ionic hydration, *in* Horne, R. A., ed., Water and aqueous solutions: New York, Wiley-Interscience, p. 597-612.

Shade, J. W., 1974, Hydrolysis reactions in the SiO_2-excess portion of the system K_2O–Al_2O_3–SiO_2–H_2O in chloride fluids at magmatic conditions: Econ. Geology, v. 69, p. 218-228.

Shettel, D. L., Jr., ms, 1974, The solubility of quartz in supercritical H_2O–CO_2 fluids: M.S. thesis, Pennsylvania State Univ., 52 p.

Shmulovich, K. I., 1969, Stability of merwinite in the system CaO–MgO–SiO_2–CO_2: Akad. Nauk. SSSR, Doklady, v. 184, p. 1177-1179.

Skippen, G. B., 1971, Experimental data for reactions in siliceous marbles: Jour. Geology, v. 79, p. 457-481.

———— 1974, An experimental model for low pressure metamorphism of siliceous dolomitic marble: Am. Jour. Sci., v. 274, p. 487-509.

Slaughter, J., Kerrick, D. M., and Wall, V. J., 1975, Experimental and thermodynamic study of equilibria in the system CaO–MgO–SiO_2–H_2O–CO_2: Am. Jour. Sci., v. 275, p. 143-162.

Sommerfeld, R. A., 1967, Quartz solution reaction: 400°-500°C, 1000 bars: Jour Geophys. Research, v. 72, p. 4253-5257.

Tödheide, K., and Franck, E. U., 1963, Das Zweiphasengebiet und die Kritische Kurve im System Kohlendioxid–Wasser bis zu Drucken von 3500 bar: Zeitschr. Physik. Chemie, Neue Folge, v. 37, p. 387-401.

Touret, J., 1977, The significance of fluid inclusions in metamorphic rocks, *in* Fraser, D. G. ed., Thermodynamics in Geology: Dordrecht-Holland, D. Reidel, p. 203-227.

Trommsdorff, V., 1966a, Beobachtungen zur Paragenese Forsterit (Klinohumit, Chondrodit) — Klinochlor in metamorphen Dolomitgestein des Lepontins: Schweizer. min. pet. Mitt., v. 46, p. 421-429.

———— 1966b, Progressive Metamorphose Kieseliger Karbonatgesteine in den Zentralalpen zwischen Bernina und Simplon: Schweizer. min. pet. Mitt., v. 46, p. 431-460.

———— 1968, The wollastonite reaction in the Western Bergell Alps: Schweizer. min. pet. Mitt., v. 48, p. 380-381.

———— 1972, Change in T–X during metamorphism of siliceous dolomitic rocks of the Central Alps: Schweizer. min. pet. Mitt., v. 52, p. 567-571.

Trommsdorff, V., and Evans, B. W., 1977, Antigorite–Ophicarbonates: contact-metamorphism at Valmalenco, Italy: Contr. Mineralogy Petrology, v. 62, p. 301-312.

Vidale, R. J., and Hewitt, D. A., 1973, "Mobile" components in the formation of calc-silicate bands: Am. Mineralogist, v. 58, p. 991-997.

Wintsch, R. P., 1975, Solid-fluid equilibria in the system $KAlSi_3O_8$–$NaAlSi_3O_8$–Al_2SiO_5–SiO_2–H_2O–HCl: Jour. Petrology, v. 16, p. 57-79.

Walter, L. S., 1965, Experimental studies on Bowen's decarbonation series III: P–T univariant equilibrium of the reaction: spurrite + monticellite = merwinite + calcite and analysis of assemblages found at Crestmore, California: Am. Jour. Sci., v. 263, p. 64-77.

Walther, J. V., and Helgeson, H. C., 1977, Calculation of the thermodynamic properties of aqueous silica and the thermodynamic properties of aqueous silica and its polymorphs at high pressures and temperatures: Am. Jour. Sci., v. 277, p. 1315-1351.

Weeks, W. F., 1956, A thermodynamic study of equilibrium relations during metamorphism of siliceous carbonate rocks: Jour. Geology, v. 64, p. 245-270.

Weisbrod, A. M., and Poty, B. P., 1975, Thermodynamics and geochemistry of the hydrothermal evolution of the Mayres pegmatite (Southeastern Massif Central, France): Petrology, v. 1, p. 1-16 and 89-102.